

ABSTRACT

Title of thesis: STRUCTURAL VARIANTS OF AI-2 TO PROBE
 BACTERIAL QUORUM SENSING IN DIVERSE BACTERIA

Sonja Gamby, Master of Science, 2011

Directed by: Assistant Professor Herman O. Sintim, Department of
 Chemistry and Biochemistry

Bacterial infections which were once easily managed with antibiotics are now reemerging as a serious threat to human health. The difficulty in managing infectious diseases is arising out of bacterial resistance to front line antibiotics. A new paradigm for fighting bacterial infection *via* the inhibition of quorum sensing has emerged. Quorum sensing is the process by which small diffusible molecules (autoinducers) are used to sense population density and upregulate genes. Notably, genes for virulence production and biofilm formation have been found to be controlled by this process. Thus, quorum sensing, offers an alternative target for the treatment of bacterial infections. One autoinducer which has been identified across many bacterial species is AI-2. The goals of this thesis were to make more hydrolytically stable analogs of AI-2 as potent inhibitors of quorum sensing, as well as, exploring the effects of AI-2 analogs on QS in *P. aeruginosa*. In this study, the processing of *bis* ester protected AI-2 analogs was examined. Also, two long chain AI-2 analogs were synthesized and tested for their ability to inhibit QS in *P.aeruginosa*. It was found that *bis* protected analogs are processed different across bacterial species. Also, long chain AI-2 analogs were found to be inhibitors of QS in *P. aeruginosa*, specifically, by inhibiting a LasR receptor which typically responds to a different class of autoinducer.

STRUCTURAL VARIANTS OF AI-2 TO PROBE BACTERIAL QUORUM SENSING
IN DIVERSE BACTERIA

by

Sonja Gamby

Thesis submitted to the Faculty of the Graduate School of the
University of Maryland, College Park, in partial fulfillment
of the requirements for the degree of
Master of Science
2011

Advisory Committee:

Assistant Professor Herman O. Sintim, Chair

Professor Jeff Davis

Professor Philip DeShong

Professor Steven Rokita

Dedication

This thesis is dedicated to my parents, Eugene and Josephine Mallory,
my children Trenton and Shiloh,
and my husband Tyrone.

Acknowledgements

I would like to thank my advisor Dr. Herman Sintim for his patience and guidance in my professional development. I would also like to thank all of my friends and family for their continued support and encouragement. I would like to acknowledge my collaborators Dr. Varnika Roy, and Dr. William Bentley and the Bentley lab. I would like to acknowledge the Maryland Pathogen Research Institute for financial support. I would also like to acknowledge my thesis committee members Dr. Jeff Davis, Dr. Philip DeShong, Dr. Steve Rokita. I would like to thank the entire staff of the University of Maryland Department of Chemistry and Biochemistry for their support. Finally, I would like to thank God for all things and acknowledge that it is by His grace that all things are possible.

Table of Contents

Dedication.....	ii
Acknowledgements.....	iii
Table of Contents.....	iv
List of Tables.....	v
List of Figures.....	vi
List of Schemes.....	viii
List of Abbreviations.....	ix
Chapter One:	
Introduction.....	1
1.1 The shift from bactericidal and bacteriostatic agents.....	1
1.2 Behaviors modulated by QS.....	2
1.3 Targeting AI-1/AI-2 signaling.....	4
1.4 Chemical synthesis of AI-1 and AI-2 analogs.....	15
1.5 Previous work and specific aims.....	19
Chapter Two: Results and Discussion.....	23
2.1 Biological activity of AI-2 analogs as ester protected compounds.....	23
2.2 Long chain analogs can modulate QS in <i>P. aeruginosa</i>	30
2.3 Preliminary results and future directions.....	35
Chapter Three: Conclusions and Future Work.....	41
3.1 Conclusion.....	41
Chapter Four: Materials and Methods, Supplemental Figures, Reference.....	44
4.1 General methods.....	44
4.2 NMR Characterizations.....	46
4.3 Methods of Biological Evaluations.....	49
4.4 Computational analysis of LasR binding.....	52
4.5 Supplementary Figures.....	52
4.6 References.....	65

List of Tables

Table 1.1: Bacterial Phenotypes under QS control.....	3
Table 2.2: Computed Binding affinities between LasR and the various forms of DPD and analogs.....	33

List of Figures

Figure 1.1: Simplified one component AHL circuit.....	5
Figure 1.2: Biosynthetic route to AI-2.....	6
Figure 1.3: Oxidative Pentose Phosphate Pathway.....	8
Figure 1.4: Biosynthesis of AHLs.....	10
Figure 1.5: Representative examples of AHLs.....	12
Figure 1.6: Single and multi-component QS circuits.....	13
Figure 1.7: <i>P.aeruginosa</i> QS circuit.....	14
Figure 1.8: Representative structures of AI-1 antagonists.....	15
Figure 1.9: First generation acyl AI-2 analogs.....	20
Figure 1.10: Second generation acyl AI-2 analogs.....	21
Figure 2.1: Compounds evaluated as <i>bis ester</i> protected AI-2 analogs.....	24
Figure 2.2: Response of enteric bacteria to <i>bis ester</i> protected AI-2 analogs.....	27
Figure 2.3: QS antagonism in <i>E.coli</i> LsrB transport mutant.....	28
Figure 2.4: Biofilm formation in <i>P.aeruginosa</i> with ester protected AI-2 analogs.....	29
Figure 2.5: Structures of nonyl and dodecyl DPD.....	31
Figure 2.6: QS response in <i>P.aeruginosa</i> in response to C9/C12 AI-2 analogs.....	31
Figure 2.7: Hydrogen bond interactions in the LasR active site.....	34
Figure 2.8: Analysis of binding mode of linear AI-2 analogs.....	35
Figure 2.9: Structural relationship between phosphorylated DPD and phospho- mimic.....	36
Figure 2.10: β -galactosidase activity in response to a molecular probe.....	40

Figure 3.1 Structural changes to C9/C12 analogs.....42

List of Schemes

Scheme 1.1: First reported synthesis of DPD and analogs.....	16
Scheme 1.2: Semmelhack's synthesis of DPD.....	17
Scheme 1.3: Doutheau's synthesis of DPD.....	17
Scheme 1.4: Vanderleyen's synthesis of DPD.....	18
Scheme 1.5: Synthesis of DPD and analogs developed in Sintim's laboratory.....	19
Scheme 2.1: Route to <i>bis</i> acetate ester DPD analogs.....	25
Scheme 2.2: Synthesis of CA-DPD.....	37
Scheme 2.3: Synthesis of MS-DPD.....	38
Scheme 2.4: Synthesis of a reactive AI-2 probe to detect QS receptors.....	39

List of Abbreviations

AHL – Acyl Homoserine Lactone

AI – Autoinducer

AI-2 – Autoinducer 2

CF – Cystic Fibrosis

DABCO - 1,4-diazabicyclo[2.2.2]octane

DBU - 1,8-diazabicyclo[5.4.0]undec-7-ene

DCM – Dichloromethane

DMDO - Dimethyldioxirane

DPD – 4,5-dihydroxy-2,3-pentadione

HSL – Homoserine lactone

Mtases – Methyl transferases

PBS – Phosphate Buffered Saline

RLU – Relative light units

R-THMF – (2R,4S)-2-methyl-2,3,3,4-tetrahydroxytetrahydrofuran

S-THMF - (2S,4S)-2-methyl-2,3,3,4-tetrahydroxytetrahydrofuran

OPNG – o-phenyl nitro pyranoside galactosidase

UPEC – Uropathogenic *Escherichia Coli*

Chapter One

Introduction

1.1 The shift from bactericidal and bacteriostatic agents

The discovery of penicillin and other antibiotics gave relief to millions of people from deadly bacterial infections. Now, a half a century later we are on the verge of returning to the pre-penicillin era, as people are continuously dying from common bacterial infections as a result of the emergence of antibiotic resistance in several clinically relevant bacteria.¹ Bacteria, and in general most cells that divide quickly (such as cancer cells) have the ability to quickly evolve to relieve environmental stress.² It is therefore not uncommon for bacteria to develop resistance within several years of being exposed to most antibiotics. Typically, the ability of bacteria to develop resistance lies in mutations. For example, a modification of only a single amino acid in the antibiotic target site can decrease the efficacy of the antibiotic (i.e. by lowering the binding affinity). Also, mutations in other enzymes can increase the degradative activity toward the antibiotic.³ With the realization that bacteriostatic or bactericidal drugs are ultimately going to be rendered ineffective by pathogens, a new paradigm regarding the treatment of bacterial infections, which does not involve the killing of bacteria, is now emerging.⁴ In the last decade, there has been a breakthrough in our understanding of the molecular details of toxin (or virulence factor) production as well as biofilm formation in bacteria.

It has now been demonstrated in a variety of bacterial species that small molecules that are used by bacteria to communicate with each other play critical roles in the expression of various virulence factors or biofilm-related genes.⁵ This phenomenon, known as quorum sensing (QS) describes the population density sensing mechanism used by bacteria. Due to its pivotal role in pathogenesis (virulence expression) and resistance (biofilm formation), quorum sensing has emerged as a valuable target for anti-infective therapy.

1.2 Behaviors modulated by QS

Virulence, or toxin production, is a key determinant in pathogenic bacteria. Many virulence factors have been shown to be under QS control.⁶ For example, pyocyanin, a virulence factor produced in *P. aeruginosa*, which inhibits cilia action and inhibits lymphocyte proliferation, is regulated by QS as well as many other virulence factors and toxins (see Table 1.1). Perhaps more importantly, biofilm production has been consistently shown to be under QS control.⁷ The ability of bacteria, both in pure and mixed cultures, to produce and thrive in biofilms likely explains why we are currently unable to permanently treat many bacterial infections. Microorganisms are able to colonize surfaces and grow as communities, known as biofilms, in which they are commonly embedded in a polysaccharide matrix.⁸ In this matrix they are more resistant to antibiotics and host defenses.

Table 1.1. Some virulence determinants regulated by QS.

Organism	Phenotype	Reference
<i>P. aeruginosa</i>	Elastase production	9
	Pyocyanin production	10
<i>E. Coli</i>	Motility	11
	Biofilm formation	12
	T3SS	13
<i>S. typhimurium</i>	InvF	14
<i>S. aureus</i>	Biofilm formation	15
<i>A. tumefaciens</i>	Gall formation	16

Biofilms have also been proposed to be associated with a range of infections including those of the gastrointestinal tract, urogenital tract, airway and lung tissue, urinary tract prostheses, catheters and other medical implants.¹⁷ For example, uropathogenic *Escherichia coli* (UPEC) invades bladder epithelial cells and forms biofilm communities.¹⁸ This behavior contributes to the difficulty in treating, and recurrence of urinary tract infections. The biofilm matrix offers a protective environment for bacteria to thrive and overcome host defenses. Biofilm-associated microorganisms are typically more resistant to antimicrobial agents, and, immune clearance and multiple factors contribute to the persistence of biofilms¹⁹. This persistence can not be overstated for those relying on medical implants or cystic fibrosis (CF) patients. *P. aeruginosa* is the leading cause for mortality in persons with CF; chronic infection and inflammation are associated with biofilm formation, a progressive decline in lung function and premature death.²⁰

This development of biofilm in *P. aeruginosa* has been demonstrated to be dependent upon QS.²¹ Also, in enteric bacteria such as *E. coli*, the *lsr* operon has been shown to regulate biofilm formation.²² Li et al. identified over a hundred genes induced by LsrR (a transcriptional regulator) and over twenty genes repressed by LsrR.²³ Two of the genes identified, *flu* and *csgE*, help mediate biofilm development (*via* control of cell-cell adhesion, and host-cell adhesion, respectively). Thus, QS is an attractive target for attenuating biofilm development and promoting clearance. *There is a scarcity of non-toxic biofilm-clearing small molecules and the development of such anti-biofilm drugs would surely ease human losses and economic burdens.*

1.3 Targeting AI-1/AI-2 signaling

Bacteria regulate their phenotypes *via* small diffusible signals called autoinducers (AIs). There are three main classes of autoinducers: autoinducing peptides (AIPs, employed by gram-positive bacteria), acyl homoserine lactones (AHLs, employed by gram-negative bacteria), and AI-2 (a signal employed by both gram-negative and gram-positive bacteria). QS circuits vary in their complexity and specific signaling molecules (AIs) utilized by bacteria. Generally, AIs are synthesized by the corresponding synthase, exported out of the cell, and detected by receptor proteins (Figure 1.1).

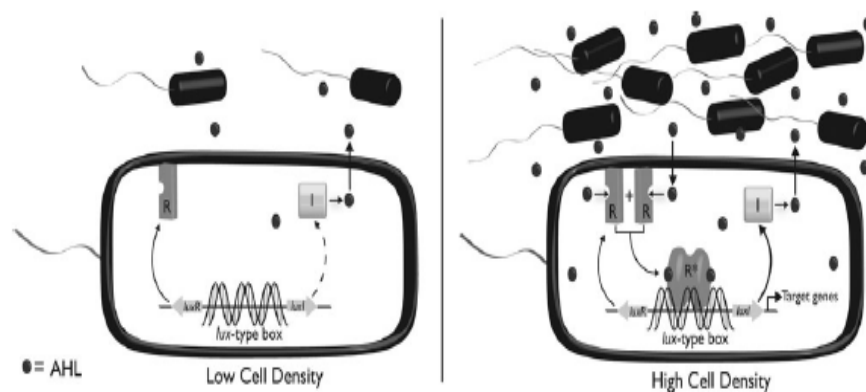


Figure 1.1. Simplified one component AHL circuit. LuxI synthesizes the cognate autoinducer while LuxR senses the AHL when the concentration reaches a threshold concentration in the cytoplasm. (Figure modified from Chem. Soc. Rev., **2008**, 37, 1432)

Biosynthesis of AI-1/AI-2

The primary biosynthetic route to AI-2 in bacteria has been established as the LuxS catalyzed production of 4,5-Dihydroxy-2,3-pentanedione (DPD) from S-ribosyl-L-homocysteine (Figure 1.2a). DPD exists as a mixture of hydration products as well as a borate complex. AI-2 is the collective term for this interconverting equilibrium mixture of compounds derived from DPD (Figure 1.2 b).

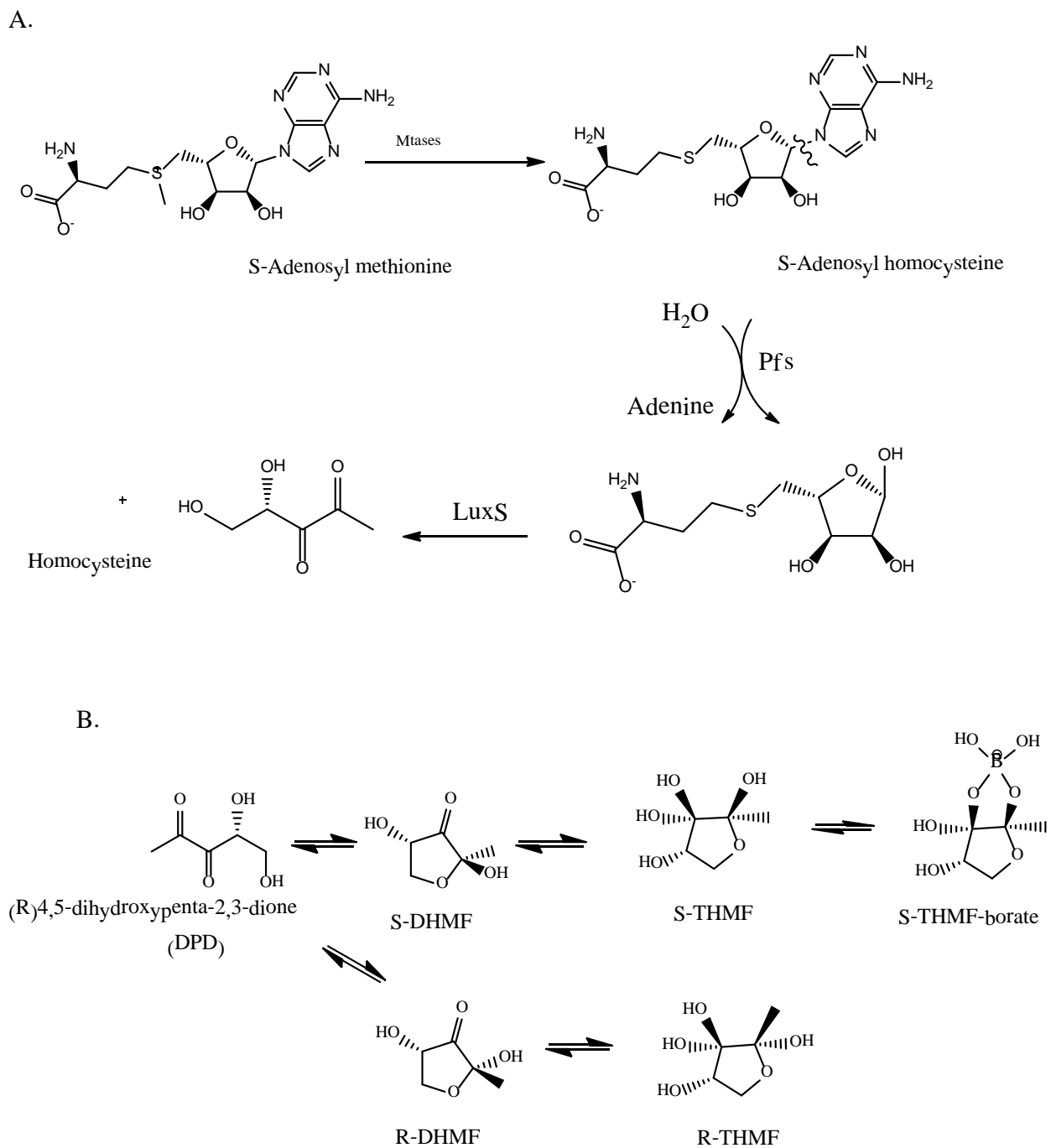


Figure 1.2 (A.) Biosynthetic route to DPD (B.) Equilibrium mixture that comprises AI-2.

Conserved *luxS* homologues exist in half of all sequenced gram negative and gram positive bacteria.²⁴ AI-2 is a dense, sugar-like metabolite, and, attention has been given to alternate biosynthetic pathways to AI-2.

It has been shown that in the presence of acid, both DPD and 4-hydroxy-5-methyl-3(2H)-furanone (HMF) spontaneously form from D-ribulose-5-phosphate (Ru5P) (Figure 1.3b).²⁵ HMF has been shown to have moderate effects on QS in *V. harveyi*. Ru5P is formed during the catabolism of glucose via the oxidative pentose phosphate (OPP) pathway (Figure 1.3a).

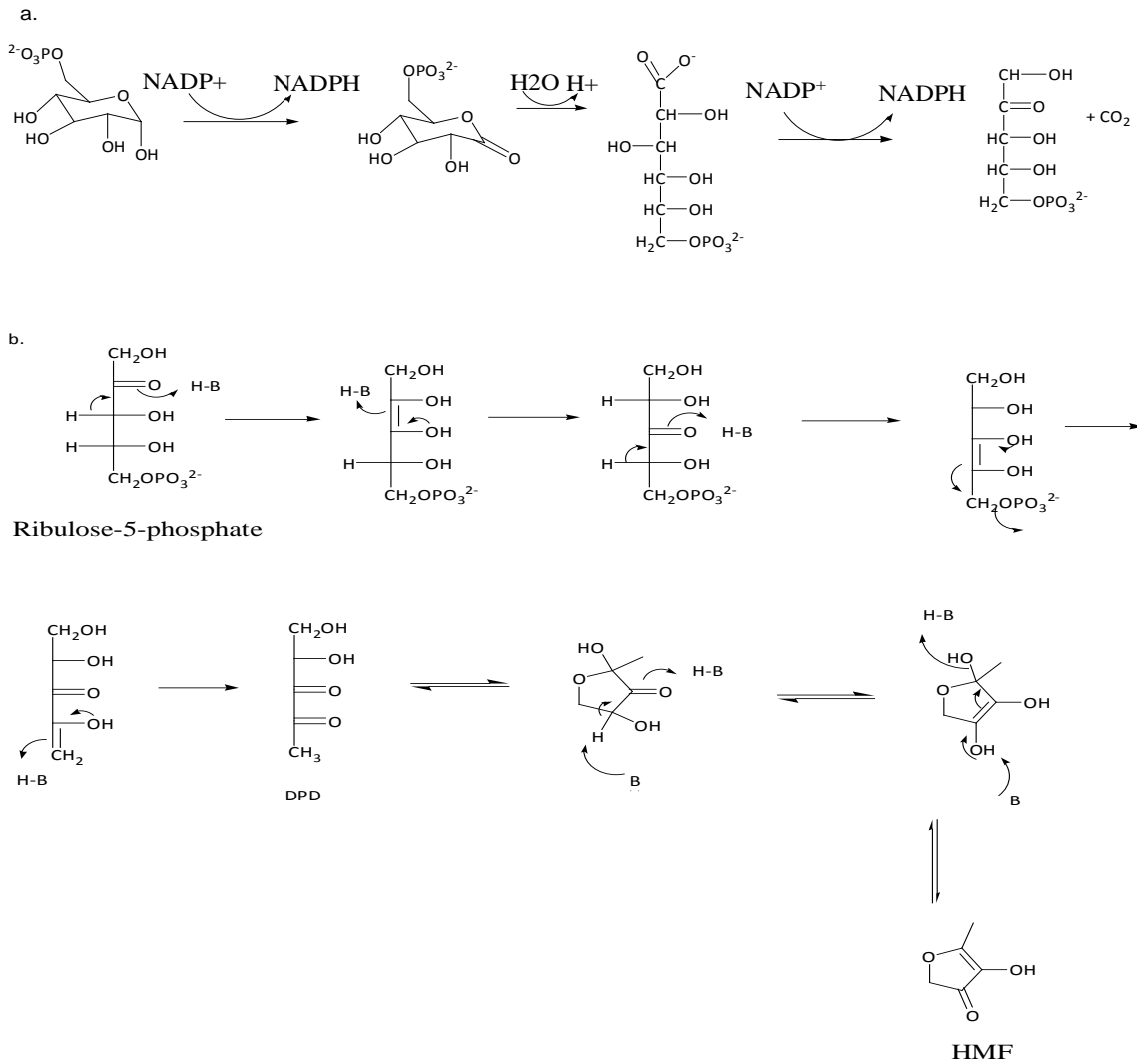


Figure 1.3 (a) Generation of D-ribulose-5-phosphate in the OPP pathway (b) Degradation pathway of Ru5P to form 4,5-dihydroxy-2,3-dipentadione and HMF.

Using an *E. coli* mutant, which degrades glucose exclusively through the OPP pathway, Tavender and coworkers showed that culture supernatants had modest activity in a *Vibrio harveyi* bioassay.²⁶ This confirmed that DPD had been generated *via* an alternative, non-enzymatic, pathway. While the OPP pathway in *E. coli* is neither effective nor necessary, it has been proposed as the pathway of choice in some species. *Phytophthora* and *Pythium* are Oomycetes lacking LuxS homology in their genome.

On the other hand, pentose phosphates are common metabolic products, and, all of the four published genomes for the *Phytophthora* species contain conserved sequences for ribose-5-phosphate (Ru5P). Kong and coworkers have shown that supernatants from these bacteria lacking *luxS* could stimulate an AI-2 mediated response (bioluminescence) in *V. harveyi*.²⁷ Nichols and coworkers have also demonstrated Ru5P as a *LuxS* independent source of DPD in the thermal-resistant bacteria *Thermotoga maritima*.²⁸ While *T. maritima* produced AI-2 it did not respond to that which was exogenously supplied. While it is clear that there are alternate biosynthetic routes to AI-2, it is also clear that there is a definite framework for the production, detection and processing of AI-2 in the canonical QS circuit. While AI-2 may serve as metabolic byproduct in some species there is much evidence supporting its role in the repression and activation of a wide range of genes.²⁹

Although it has been shown that not all bacterial species that produce AI-2 utilize AI-2 in QS, the function of AHLs is attributed solely to QS. AHLs are synthesized *via* members of the LuxI family which use the appropriately charged acyl-acyl carrier protein (acyl-ACP) and *S*-adenosylmethionine as the sources of the acyl side chain and the homoserine lactone (HSL) ring, respectively (Figure 1.4).³⁰

Bacterial genome databases now contain more than 100 different LuxI homologues, though few show high protein sequence homologies.³¹ While this is in direct contrast to LuxS, this observation is not surprising, as the products of LuxI are highly variable.

Interestingly, the biosynthesis of AHLs is not exclusively dependent on LuxI homologues.

The LuxM family of AHL synthases, has been identified in *Vibrio harveyi*³² and other *Vibrio* species.³³ Also, a third potential AHL synthase (HdtS) which does not belong to either the LuxI or LuxM families has been identified.³⁴

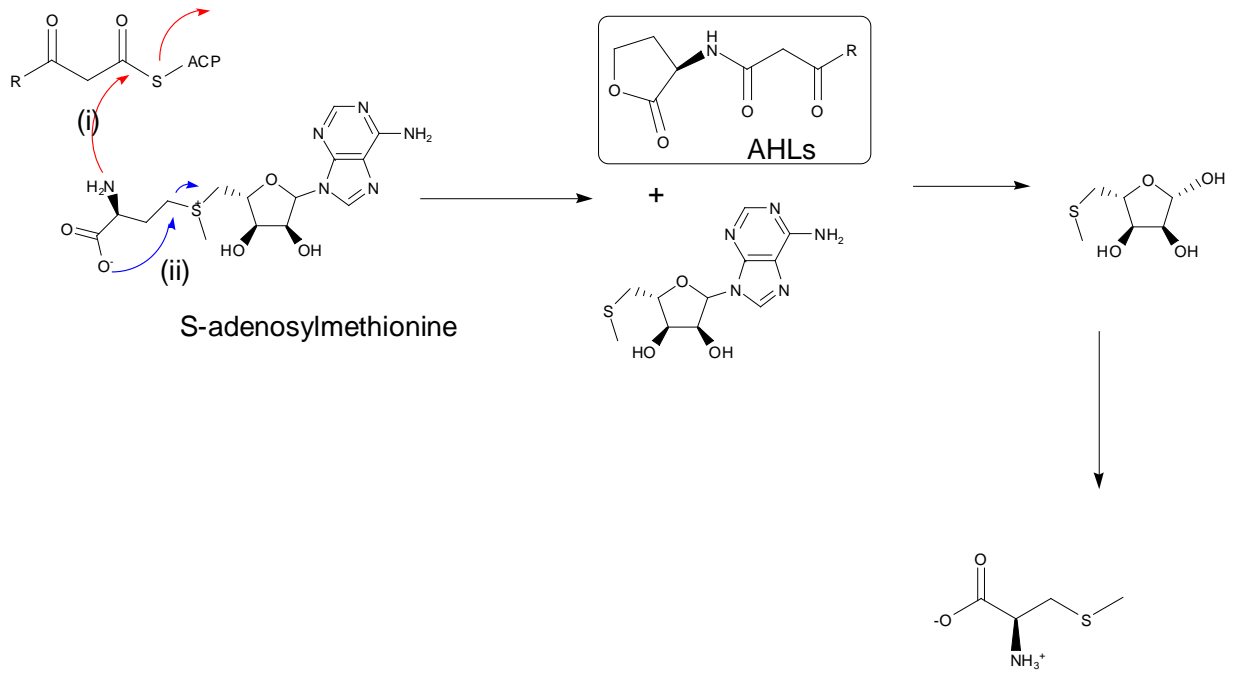


Figure 1.4. Biosynthesis of AHLs.

QS Circuits in gram-negative bacteria

Gram-negative QS bacteria typically utilize AHLs as AIs, with bacterial species detecting the accumulation of one or more AHL molecules. These AHL signaling molecules vary between species as a function of their oxidation state as well as their acyl chain length (Figure 1.5).

As previously discussed, the secretion of AHLs is governed by the synthase LuxI and the detection of AHLs occurs *via* diffusion across the cell membrane and detection by LuxR type proteins. In the absence of AHLs LuxR is an insoluble protein which rapidly degrades.³⁵ The presence of AHLs promotes the folding and subsequent dimerization of LuxR. This LuxR:AHL complex then goes on to bind to DNA where it regulates the expression of many genes.³⁶ The LuxI/R system described above refers to a cytoplasmic receptor protein, LuxR. Gram-negative bacteria can also utilize membrane-bound receptors, designated as LuxN type.³⁷ In these systems, the synthase, LuxM is responsible for the production of its cognate signaling molecule.³⁷ This signal reaches a threshold concentration in the periplasm where it is detected by a LuxN-type two component histidine kinase.³⁸ The binding of AHL to LuxN initiates the reversal of a phosphorelay, thereby de-repressing the transcriptional regulator, LuxR (Figure 1.6a).³⁸ Another AI used by both gram-negative and gram-positive bacteria alike is AI-2.⁴⁷

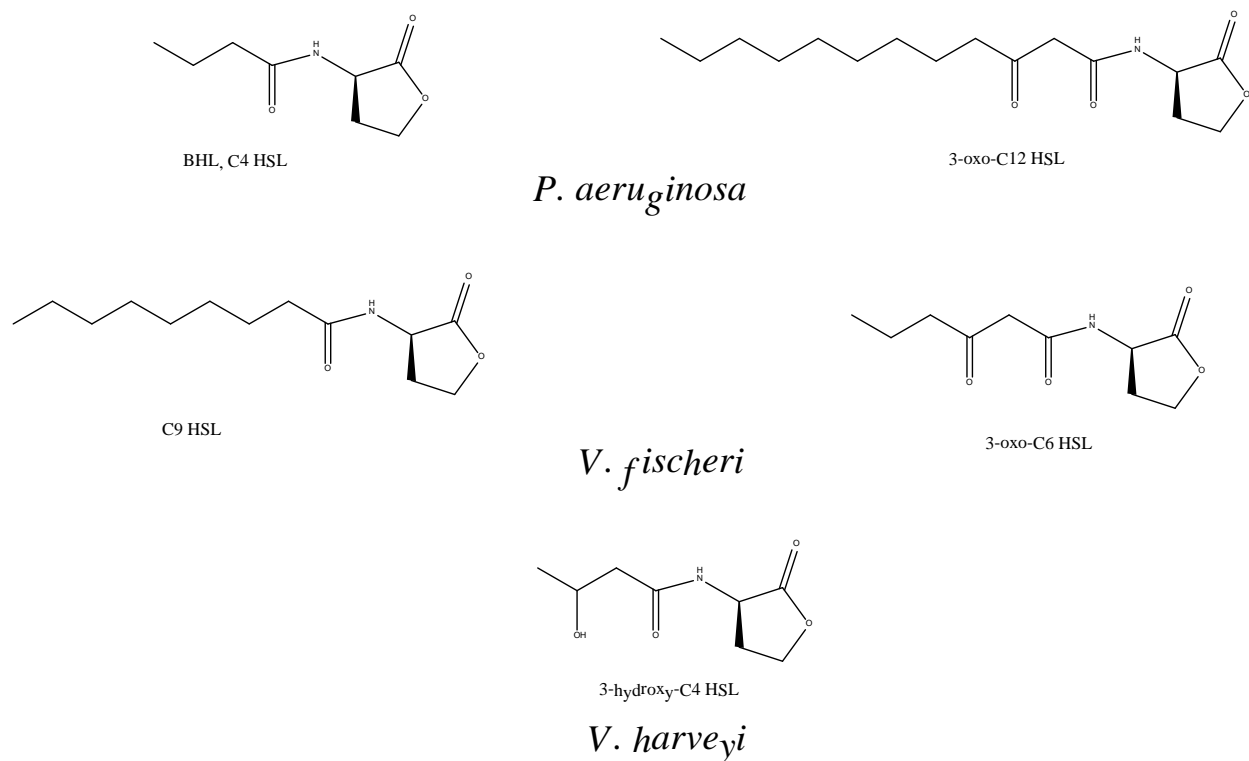


Figure 1.5. Some representative examples of AHLs used by various species.

Mechanisms for the internalization of AI-2 vary between species. AI-2 is produced by a conserved synthase LuxS, however, receptors for the various forms of AI-2 differs between species. For example, *Vibrio harveyi* recognizes S-THMF via a LuxPQ histidine-kinase³⁹, while *Salmonella typhimurium* utilizes an ABC type transporter which recognizes R-THMF and imports it into the cytoplasm.⁴⁰ Once in the cytoplasm, the linear form of AI-2 (DPD) is phosphorylated by LsrK⁵², the product, Phospho-AI-2, then binds to the transcriptional regulator LsrR (Figure 1.6b).⁵² Multiple QS circuits don't always act synergistically as in *V. harveyi*. *Pseudomonas aeruginosa* utilizes three distinct signals and four receptors which either activate or antagonize each other (Figure 1.7).⁴¹

Knowledge of the various circuits is crucial to intercepting QS; molecular probes can potentially identify key receptors, elucidate their roles in signaling relays, and, aid in the design of potent antagonists.

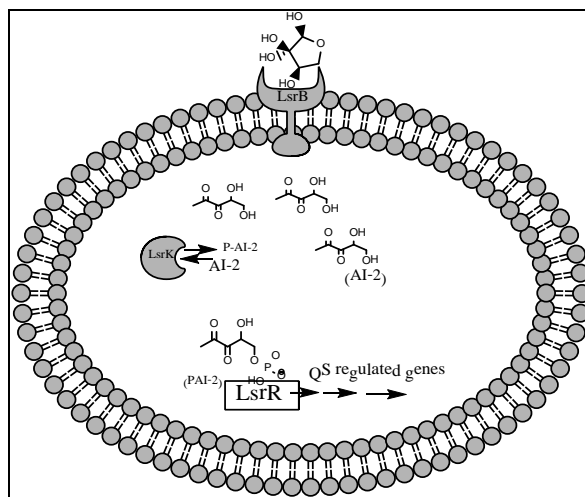
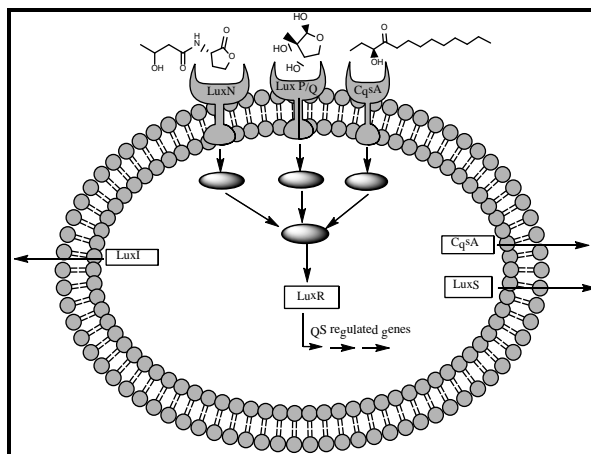


Figure 1.6. Single and multi-component QS circuits (a) QS circuit of *V. harveyi*. The three AIs initiate phosphorelays that feed into the same phosphorylated \square cascade and activate the transcriptional regulator. (b) QS circuit of *S. typhimurium*. A cyclic form (R-THMF) of AI-2 is transported across the cellular membrane, enters the cytoplasm and becomes phosphorylated by LsrK. This Phospho-AI-2 complex binds to and activates the transcriptional regulator.

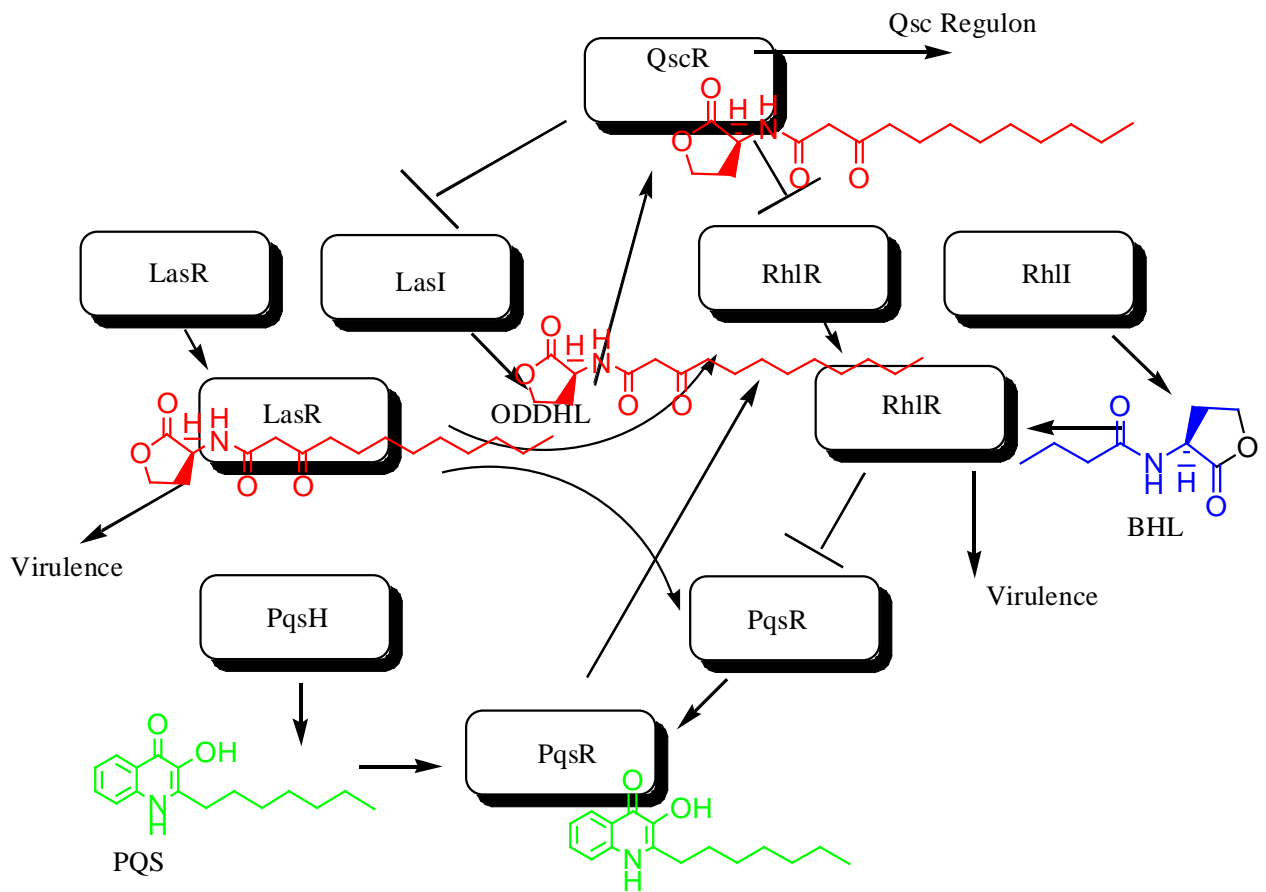


Figure 1.7. *P. aeruginosa* QS circuit. Flattened arrows indicate negative regulation while pointed arrows indicate upregulation of the corresponding gene(s).

A popular approach to attenuating QS has been through the inhibition of receptor proteins.⁴² Toward this end, there have been many AI analogs reported for their efficacy in the inhibition of QS (Figure 1.8).⁴³

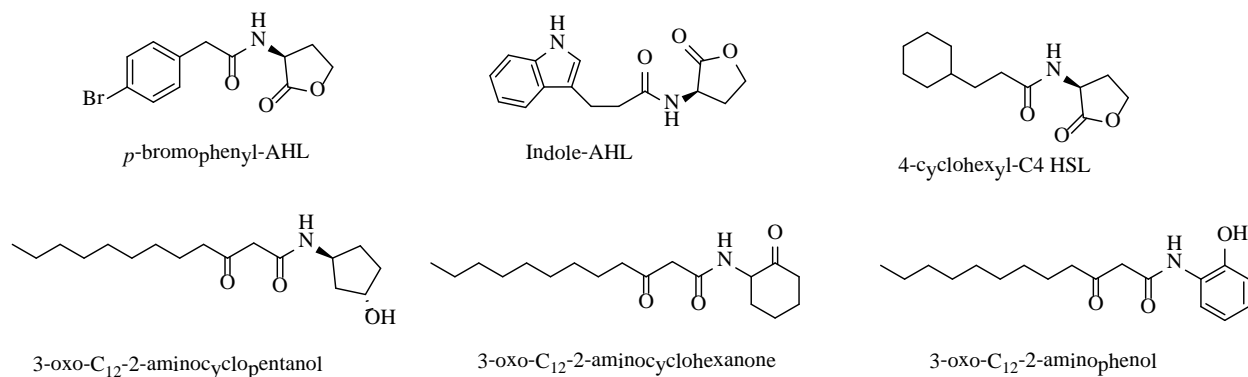


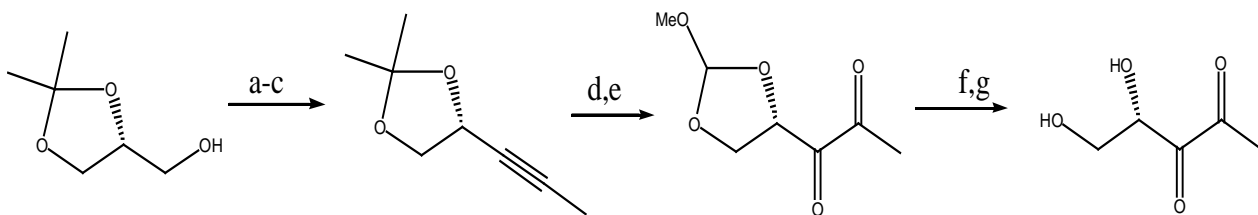
Figure 1.8. Representative structures of AI-1 analogs with QS inhibitory activity⁴⁴

Over two decades ago, Eberhard and coworkers reported AHL analogs possessing potent QS inhibition activities.⁴⁵ Since then, many other groups have developed analogs and novel synthetic methods for arriving at vast libraries of potential antagonists.⁴⁶ Despite these massive efforts by several groups, there are still no anti-virulence or anti-biofilm drugs in clinical use as of today. One autoinducer that shows great promise is the so-called ‘universal’ autoinducer AI-2, as the various forms of AI-2 are recognized by over seventy species of bacteria.⁴⁷ A few groups have synthesized analogs of AI-2 which have been shown to interfere with quorum sensing in enteric bacteria.⁴⁸ Additionally, AI-2 analogs have been shown to inhibit virulence factor production as well as biofilm formation.⁴⁹

1.4 Chemical Synthesis of AI-2 and AI-2 Analogs

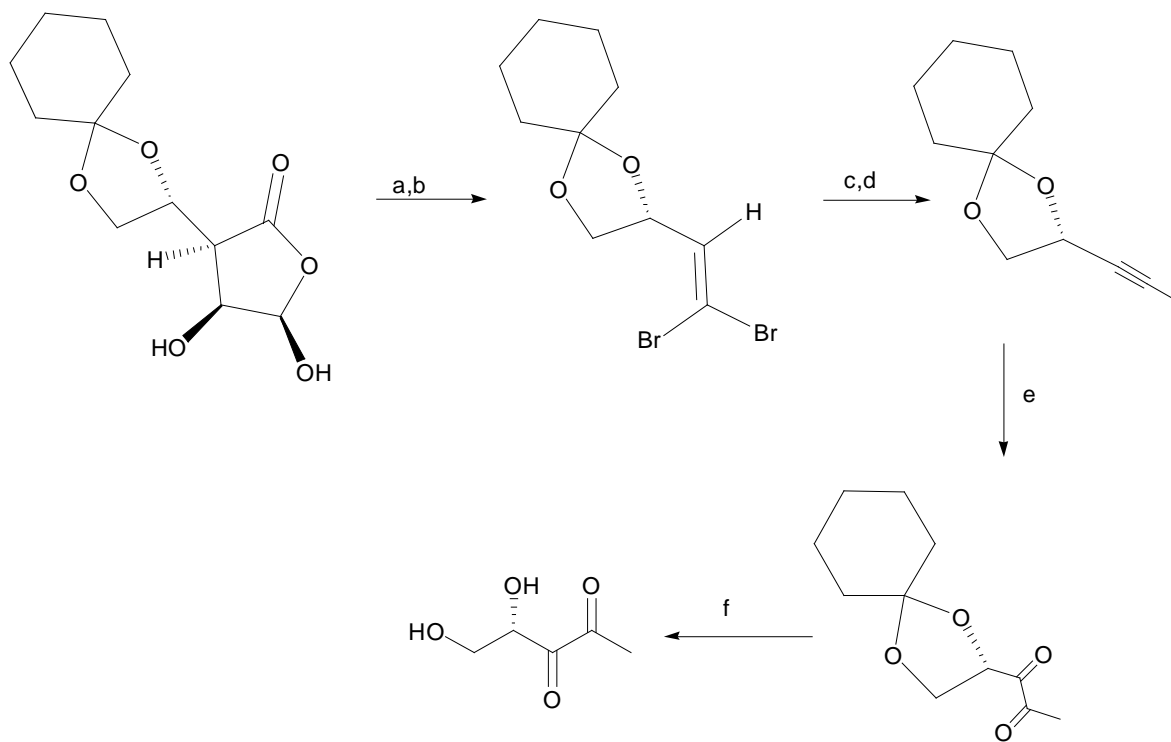
While several groups have reported various AI-1 analogs that are effective QS inhibitors, the development of AI-2 analogs lags behind.

Over the last decade there have been numerous reported syntheses of AI-2 and AI-2 analogs. Notably, the first synthesis of AI-2 was accomplished by Janda's group in 2004 (Scheme 1.1).⁵⁰ This synthesis was based upon an acetal protected alkyne, **2**. Oxidation of **2** and subsequent deprotection yielded AI-2 and alkyl analogs in moderate yields. Here, functionalization was achieved during the Corey-Fuchs homologation *via* the selection of various alkenyllithium alkyldonors, thus, the access to C1 analogs was limited. Variations of Janda's synthesis were later published with the difference being either (1) selection of protection groups⁵¹ or (2) route to the diketone moiety.^{45,52}



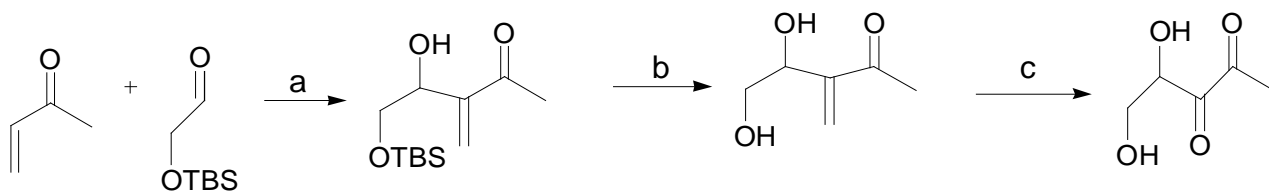
Scheme 1.1. First reported synthesis of DPD and analogs. Reagents and conditions: a. Oxayl chloride, dimethyl sulfoxide, dichloromethane; triethyl amine; b. CBr_4 , triphenyl phosphine, dichloromethane; c. *t*-butyl lithium, methyl iodide, tetrahydrofuran; d. 60% acetic acid; e. $\text{CH}(\text{OMe})_3$ (neat), H_2SO_4 (cat); f. KMnO_4 , acetone buffer (aq); g. H_2O , pH 6.5 ($\text{K}_2\text{HPO}_4/\text{KH}_2\text{PO}_4$ (0.1M), NaCl (0.15M)), 24 H.

Shortly after Janda's synthesis, Semmelhack published a similar synthesis involving a cyclohexylidene protecting group for the diol, and a lactone precursor to the requisite aldehyde for the Corey-Fuchs reaction (Scheme 1.2).⁴⁵



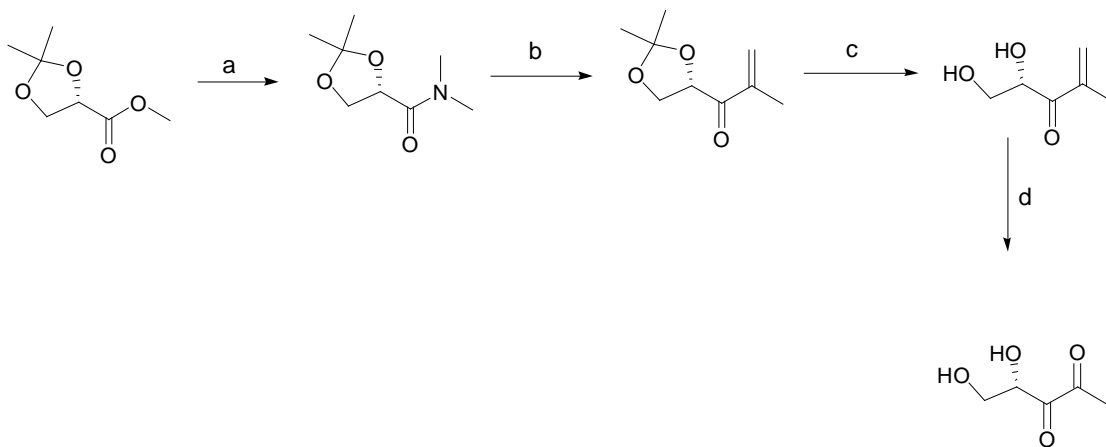
Scheme 1.2. Semmelhack's synthesis of DPD. Reagents and conditions: (a) KIO_4 , K_2CO_3 , $\text{H}_2\text{O}/\text{CH}_2\text{Cl}_2$ (b) Ph_3P , CBr_4 (c) 1. *n*-BuLi, 2. H_2O (d) 1. *n*-BuLi 2. CH_3I (e) RuCl_2 (cat.), NaIO_4 (f) pH 1.5.

Doutheau published a short, three step synthesis of AI-2 based on the Baylis-Hilman reaction (Scheme 1.3).⁵³ Yet, the enone required to add to the aldehyde is not commercial, so this methodology *en route* to AI-2 analogs is limited and would require additional steps.



Scheme 1.3. Doutheau's synthesis of DPD. Reagents and conditions: (a) THF, DABCO, 0°C (b) TBAF/THF, RT (c) 1. O_3 , MeOH, -78°C 2. DMS, -78°C to RT.

Lastly, Vanderleyen utilized the familiar acetal group to obtain the diol functionality and the coupling of a Grignard and an amine to access the α,β -unsaturated carbonyl which is subsequently oxidized (Scheme 1.4).⁴⁶

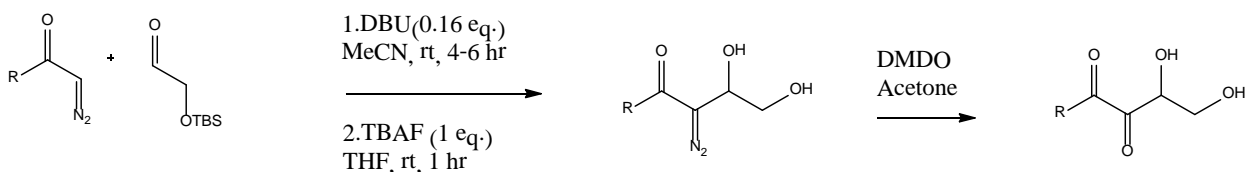


Scheme 1.4. Vanderleyen's synthesis of DPD. Reagents and conditions: (a) $\text{NH}(\text{CH}_3)_2$, EtOH (b) $\text{CH}_2=\text{CCH}_3\text{MgBr}$, $\text{Et}_2\text{O}/\text{THF}$ (c) DOWEX resin, MeOH (d) O_3 , MeOH, DMS

While syntheses of AI-2 continue to be published, the underlying problem with most is that most reported syntheses are not facile enough to readily generate diverse AI-2 analogs from commercial starting materials. In 2009, the Sintim group developed a facile, two-flask synthesis that is amenable to the generation of a variety of C1 AI-2 analogs (Scheme 1.5).⁵⁴

The key step in Sintim's synthesis is the carbonyl condensation between various diazocarbonyls and a commercially available 2-(*t*-butyldimethylsiloxy) acetaldehyde. Both alkyl and cyclic diazocarbonyls could be obtained from the requisite acid chloride and acyldiazomethane.

The diazo diol intermediates were obtained through deprotection with *tetra*-butyl ammonium fluoride. Column chromatography purification of the diazo diol followed by oxidation with dimethyl dioxirane resulted in pure DPD in moderate to high yields. To date this synthesis has produced 22 AI-2 analogs with linear, branched, cyclic, and, aromatic C1 groups.



Scheme 1.5. Synthesis of DPD and analogs developed in Sintim's laboratory. DBU = 1,8-diazabicycloundec-7-ene, TBAF= tert-butyl ammonium fluoride, THF = tetrahydrofuran, DMDO = dimethyldioxirane.

1.5 Previous work and Specific Aims

A previous student in the Sintim group, Jacqueline Smith, investigated whether AI-2 analogs with the acyl chain modified could be used to antagonize AI-2 signaling in a variety of bacteria (Figure 1.9).

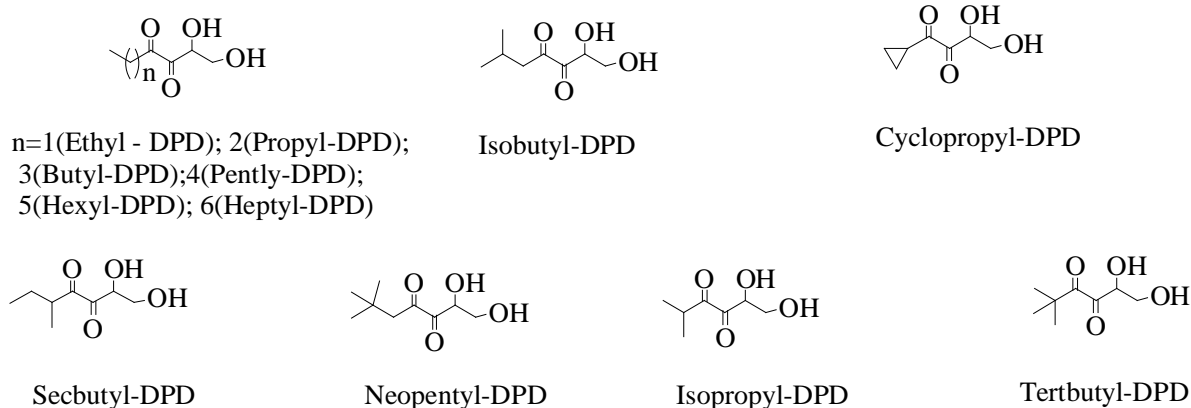


Figure 1.9. First generation of C1 AI-2 analogs.

The conclusion of these studies was that the nature of the C1 alkyl group affected which bacteria could be targeted. For example, butyl-DPD inhibited AI-2 signaling in *E.coli* but not *S.typhimurium*, whereas isobutyl-DPD inhibited both species.

In collaboration with Drs. Jacqueline Smith and Varnika Roy, I synthesized an expanded set of AI-2 analogs (Figure 1.10). The aim for the synthesis of these second generation analogs was to identify new specific inhibitors for other bacterial species and also to investigate if these analogs could be used to specifically inhibit bacteria in an ecosystem. One of the species targeted during the study was *Pseudomonas aeruginosa*; this organism is extremely devastating to immuno-compromised individuals. Though typically known for its LasI/LasR QS circuit (responsive to AI-1 type autoinducers), it has been shown that virulence production in *P.aeruginosa* is enhanced by AI-2 derivatives.⁵⁵ We found that phenyl-DPD could inhibit the virulence factor (pyocyanin) production in *P. aeruginosa* while QS in *E.coli* and *S. typhimurium* was unaffected.

Also, when isobutyl-DPD and phenyl-DPD were used as a cocktail in a synthetic ecosystem (comprising *E. coli*, *S. typhimurium*, and *P. aeruginosa*), the specific antagonistic activity was retained. This recent observation that in mixed cultures, organisms can be selectively targeted is very powerful. It is conceivable, for example, that *P. aeruginosa* could degrade isobutyl DPD though it is not antagonized by the compound. For example, *S. typhimurium* possesses the degradation proteins LsrF and LsrG which accelerate processing of DPD; these enzymes have not been identified in *E. coli* (though the QS circuits are highly homologous).⁵⁶ The identification of these specific QS inhibitors is exciting; however, one unanswered question is whether these DPD analogs are acting *via* the AI-1 pathway or through an unknown pathway. Also, DPD and analogs are generally unstable therefore, new ways to make stable AI-2 analogs are needed.

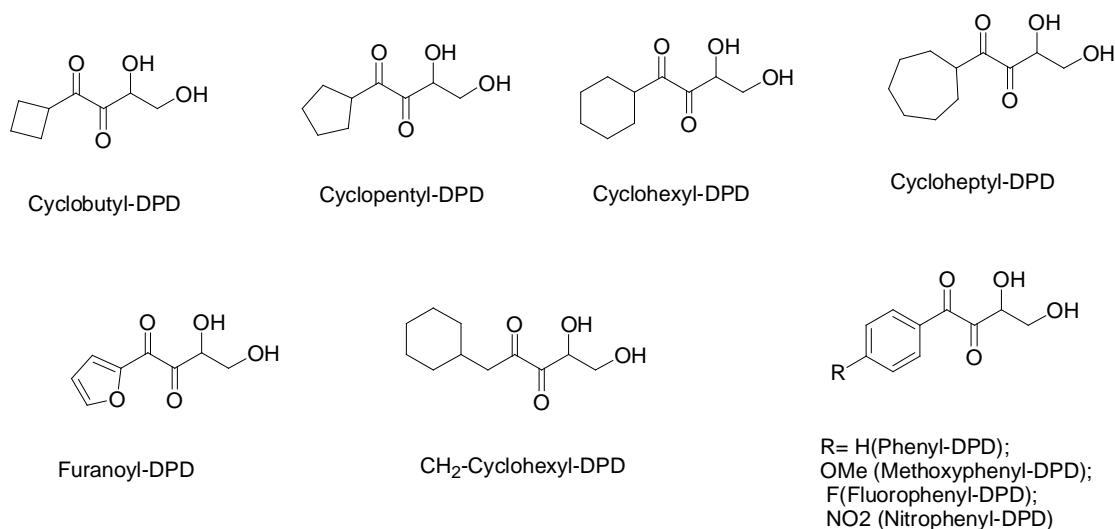


Figure 1.10. Second generation AI-2 analogs.

The specific aims of this thesis are (i) the synthesis of pro-AI-2 analogs that are stable and can be unmasked in bacterial cells (ii) to synthesize DPD analogs that are ‘AI-1 like’ (i.e. having long, linear hydrophobic acyl chains) and investigate if these analogs are capable of acting on the AI-1 pathway in *P. aeruginosa*.

Chapter Two

Results and Discussion

2.1 Biological Activity of AI-2 Analogs as Ester Protected Compounds

While AI-2 analogs can inhibit QS circuits, AI-2 analogs are not themselves viable drug candidates. The instability of these analogs would likely contribute to their premature degradation in the human body. From a practical standpoint, AI-2 analogs are not easily purified, thus, any large scale production of these analogs mandates that modifications be made. In 2007, Doutheau reported that DPD *bis* acetate esters were stable precursors of DPD.⁵⁷ It is presumed that esterases inside bacterial cells can cleave the ester moiety to yield biologically active DPD. The activity of these ester protected DPD compounds was determined by the ability of the compounds to induce β -galactosidase production in *E.coli* and *S. typhimurium* as described below. Briefly, the Lsr (**L**ux **S** **R**egulated) operon is appended with a gene encoding β -galactosidase. When the Lsr operon is expressed (*via* AI-2 induced derepression of LsrR), the β -galactosidase enzyme is expressed as well. When the chromogenic substrate, O-PNG, is added to cultures with varying levels of enzyme, the cleavage product can be observed at 420 nM and used as a measure of activity. While Doutheau's study confirmed the use of *bis*-methyl ester protected DPD as an agonist, it did not discuss the antagonistic profile of AI-2 analogs nor examine the use of various ester protecting groups.

One of the aims was to make various ester-protected DPD analogs and determine which ester protection was optimal for the induction of the QS response. Secondly, we aimed to determine if ester protected DPD antagonists such as isobutyl-DPD and hexyl-DPD, could be protected as esters and retain their inhibitory activity.

Synthesis of various bis ester protected DPD analogs

A series consisting of methyl, propyl, butyl, and pentyl *bis* ester DPD analogs was desired in order to compare the effects of ester chain length on permeability. Presumably, ester analogs of AI-2 chains would be more stable towards retro-Aldol degradation and hence would be easier to purify on silica gel. Methyl-DPD, hexyl-DPD and isobutyl-DPD were chosen as analogs to convert into their ester forms (Figure 2.1). All compounds were synthesized following protocol developed in the Sintim lab (Jacqueline A.I. Smith, PhD dissertation, University of Maryland, 2011)⁵⁸ (Scheme 2.1). With these analogs in hand, we proceeded to test their activity in *E.coli* and *S.typhimurium* using the β -galactosidase assay previously described.

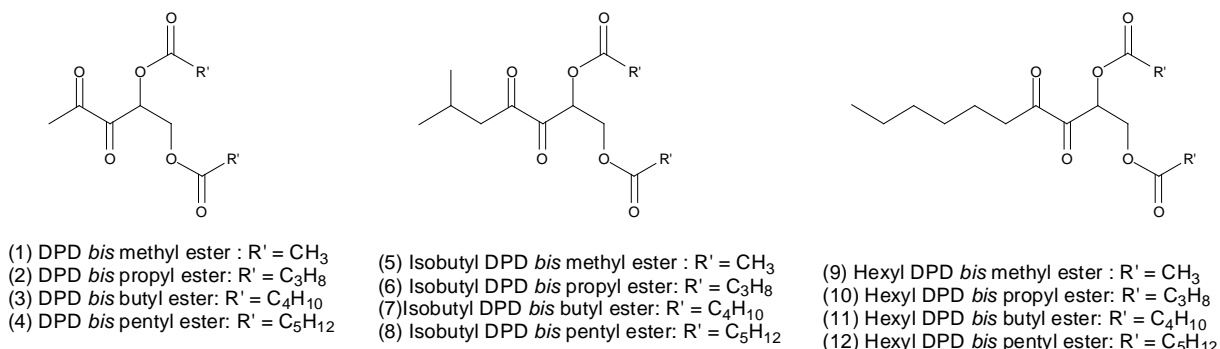
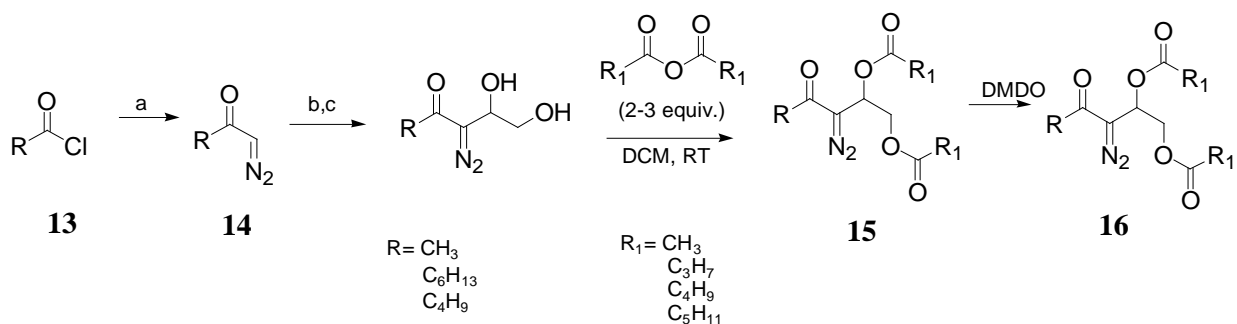


Figure 2.1. Compounds evaluated as *bis* ester protected AI-2 analogs.



Scheme 2.1. Reagents and conditions: (a) diazomethane, 0°C, (b) *t*-butyl-dimethylsiloxylaldehyde, 1,8 diazabicycloundec-7-ene, CH₃CN, RT (c) TBAF/THF. DCM= dichloromethane; DMDO= dimethyldioxirane.

Ester Protected DPD analogs are processed differently in E.coli and S. typhimurium

In *E. coli* DPD, *bis*-methyl, propyl, butyl and pentyl esters are able to induce the expression of the *lsr* operon. In contrast, *S. typhimurium* is unable to process *bis* esters as efficiently, displaying only moderate levels of *lsr* expression (Figure 2.2a). In *E. coli*, the methyl and propyl *bis*-ester derivatives of isobutyl-DPD are effective, while the *bis* esters are generally unable to inhibit QS in *S. typhimurium* (Figure 2.2b). Possible reasons for the divergent activity are (1) membrane permeability varies between the two species, or, (2) the selectivity of esterases varies between the species. Membrane permeability assays of the ester protected analogs could shed light on these observations.

Both *E. coli* and *S. typhimurium* contain the LsrACDBF(G)E operon (with *E. coli* lacking the *lsrG* gene). The LsrACBD components comprise an ABC transporter protein.

LsrB has homology to periplasmic ribose proteins and it is proposed that the role of LsrB is to bring AI-2 into contact with the channel and ATP components of the Lsr transporter (predicted to lie in the inner membrane).⁵⁹

Also, while LsrACBD is critical for AI-2 uptake in *Salmonella*, it is not necessary in *E. coli*. Interestingly, when isobutyl-DPD *bis* esters were evaluated in LsrB mutants, the observed antagonism exceeded both that of *E. coli* and *Salmonella* (Figure 2.3).

In *E. coli*, the fact that all methyl DPD *bis*-esters (**8a-d**) are capable of agonism and only isobutyl DPD esters up to propyl (**9a-c**) can antagonize indicates that the C1 side chain also plays a role in the ability of analogs to either cross the cellular membrane or be unmasked by esterases. Further experiments are needed to resolve this issue.

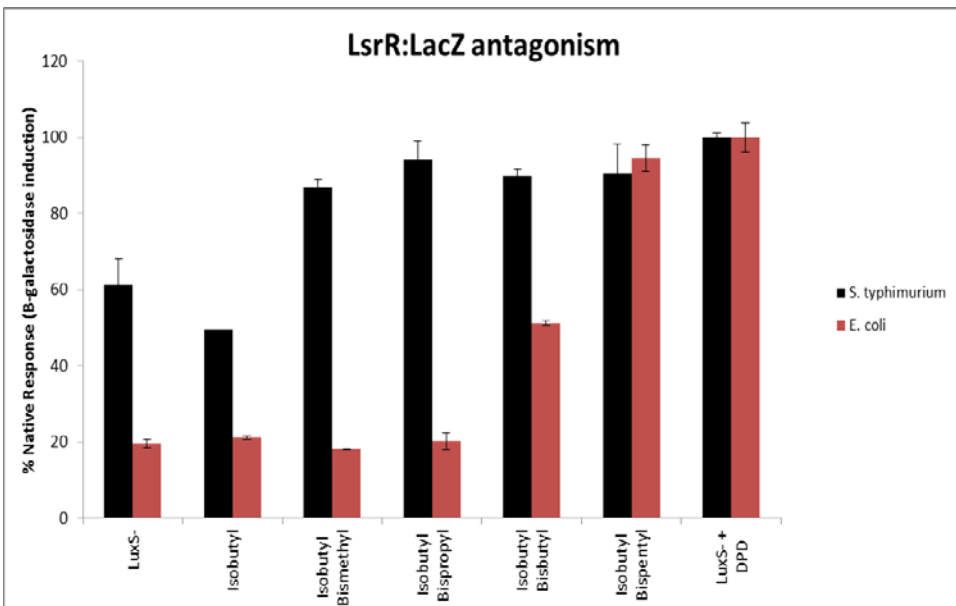
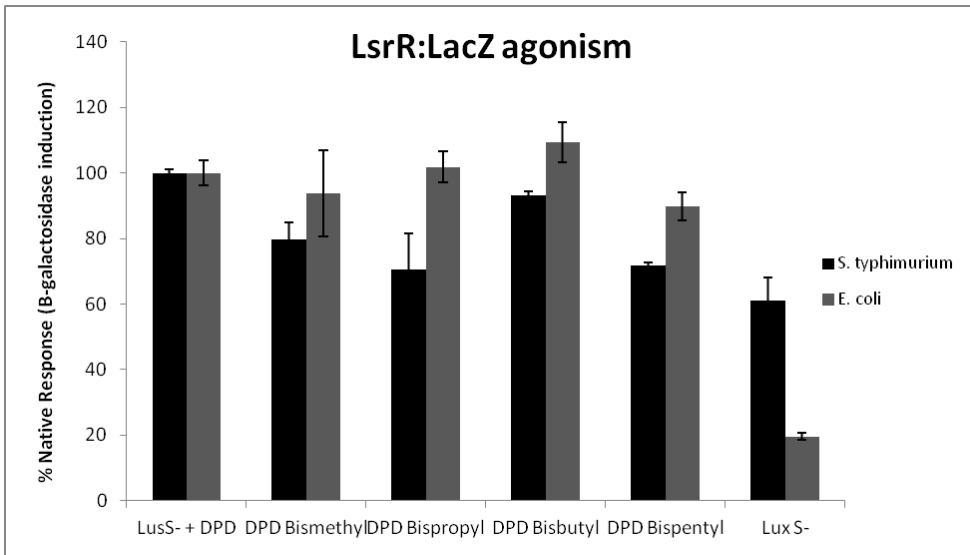


Figure 2.2(a). Response of enteric bacteria to *bis*-ester protected AI-2 analogs (Top) Agonism in *S. typhimurium* (MET715, LuxS-) and *E. coli* (LW7, LuxS-) in response to 20 μ M *bis*-ester AI-2. (b)(Bottom) Antagonism in LuxS- *S. typhimurium* and *E. coli* supplemented with exogenous AI-2 (20 μ M) and 20 μ M *bis*-ester DPD analogs.

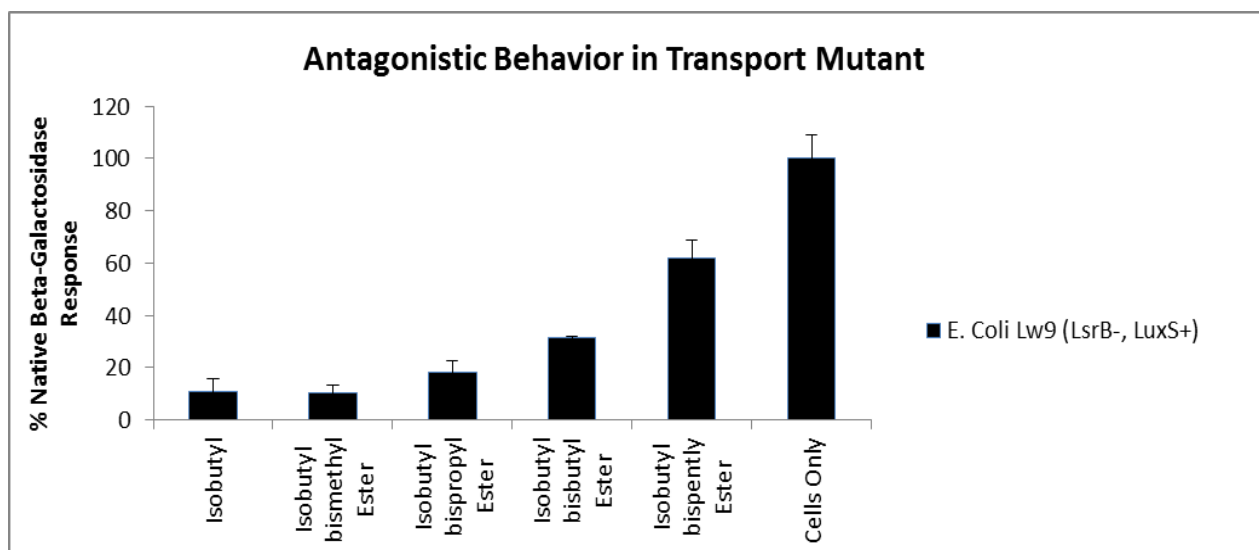


Figure 2.3. Antagonism in LsrB- *E. coli* exceeds that of the strain with an intact transporter.

Ester protected DPD analogs as QS inhibitors in P.aeruginosa

Acetate protected AI-2 analogs contain the long acyl-chain moiety present in AHLs. Thus, we wondered if acetate protected analogs could interfere with QS in *P. aeruginosa*. To probe the effect of acetate protected AI-2 on *P.aeruginosa*, the effect on biofilm formation was measured. *P. aeruginosa* (PAO1) was grown both in isolation, and in the presence of AI-2 analogs.

After 24 hours, biofilm was measured *via* crystal violet staining and quantified as the absorbance at 550 nm (Figure 2.4).⁶⁰

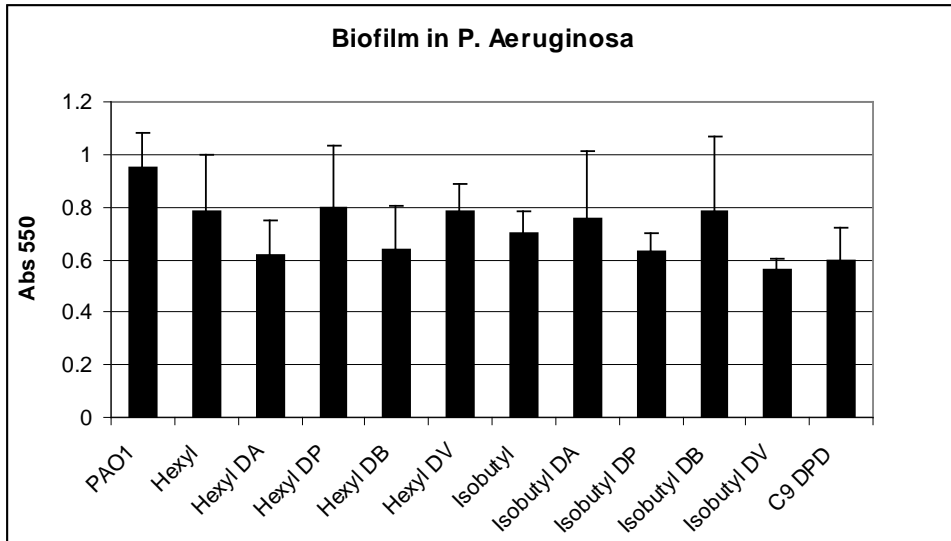


Figure 2.4. Effects of ester protected AI-2 compounds on the ability of *P.aeruginosa* to form biofilm.

While static biofilm measurements are highly variable, we were encouraged that AI-2 analogs could not only modulate QS in *E. coli* and *S. typhimurium*, but in *P. aeruginosa* as well.

2.2 Long chain AI-2 analogs can modulate QS in P.aeruginosa

P. aeruginosa produces virulence factors in response to AI-2 though it itself does not harbor the requisite synthase to make AI-2.⁶¹ We and others⁶² have observed moderate inhibition of QS in *P. aeruginosa* in response to AI-2 analogs. Ganin et al. have shown that both Pentyl and Hexyl DPD inhibit the lasR:LasI QS circuit. As LasR type proteins recognize their respective signaling molecules as a function of chain length, we wondered if longer chain AI-2 analogs would be more potent antagonists. The native AHL of *P. aeruginosa*, 3-oxo-dodecanoyl-HSL, contains an acyl chain 12 carbons long. We reasoned that as the C1 chain length increased to that of the native ligand, affinity to LasR would also increase. Towards this end, nonyl and dodecyl DPD were synthesized according to our previously published method (Figure 2.5). These long chain AI-2 analogs were tested with a bioluminescent LasR:LuxCDABE reporter strain (PAO1 PSB1075)⁶³. This strain is deficient in the requisite AHL synthase (LasI) and displays luminescence in response to LasR activation. *P. aeruginosa* was cultured with 20 μ M 3-oxo-dodecanoyl HSL and 40 μ M nonyl or dodecyl DPD and bioluminescence was observed every hour for eight hours. The maximal response was observed after 5 hours. Approximately 50% inhibition of bioluminescence was observed in both long chain analogs; interestingly, there is an increase in the efficacy of the analogs with an increase in the chain length of C1 (Figure 2.6). As AI-2 exists as an equilibrium mixture of products, we wondered if one intermediate was more effective than the rest. The receptor protein LasR has been co-crystallized with its cognate HSL.⁶⁴

To both confirm our observations and identify the most effective form(s) of AI-2 analogs, we performed a computational analysis of LasR-AI-2 binding.

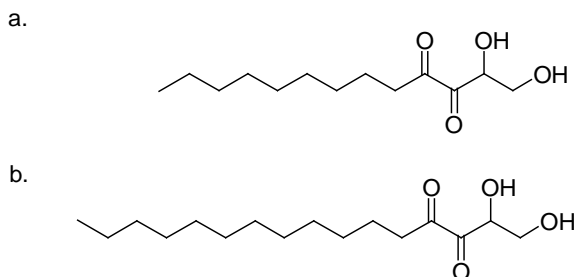


Figure 2.5. Structures of nonyl (a) and dodecyl (b) DPD.

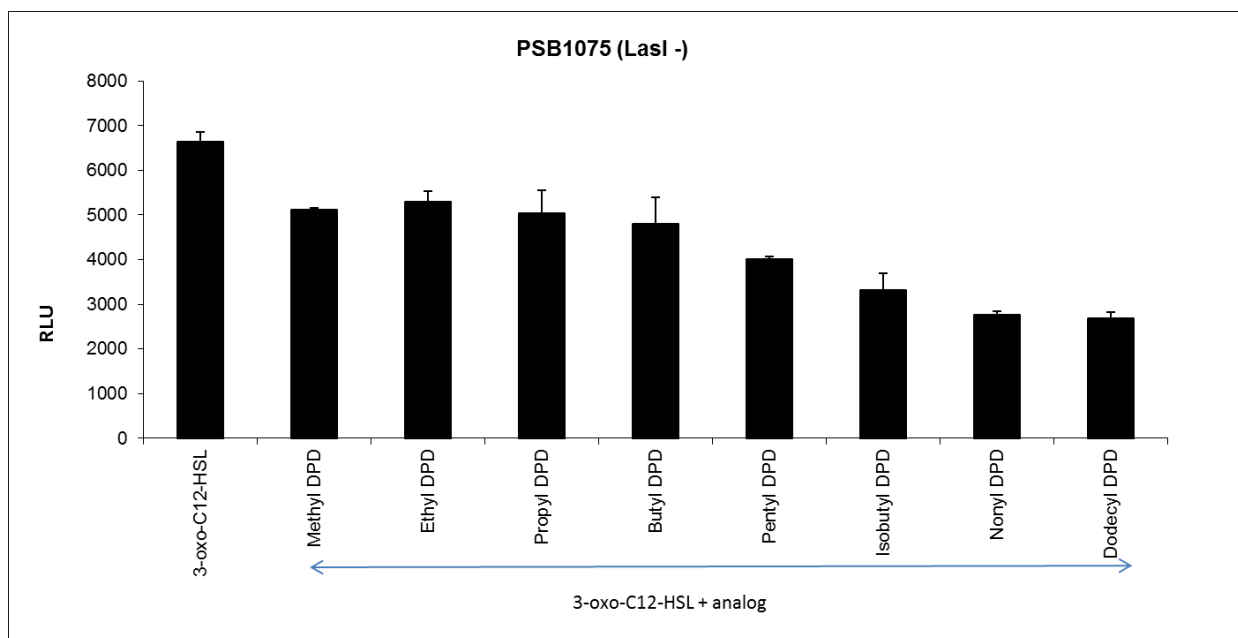


Figure 2.6. QS response in *P. aeruginosa* in response to long chain AI-2 analogs (RLU = relative light units).

Computational Analysis of LasR Binding with AI-2 Analog

AutoDock Vina⁶⁸ was used to model protein-ligand interactions and rank their binding affinities. LasR complexed with its native ligand, 3-oxo-C12-HSL (PDB ID = 3IX3) was used as the receptor protein. Autodock Vina is a widely used docking software which scores protein-ligand interactions on the basis of the free energy differences between the bound and unbound state. Solvent effects are neglected. All calculations were done with an exhaustiveness of 64.

Consistent with biological observations, the binding affinities increased as a function of chain length (Table 2.1). Among the cyclic forms, there does not appear to be much preference for hydrated over the cyclic ketone form. In general, cyclic forms confer slightly higher binding affinities. There is a -3.2 kcal/mol increase from DPD to dodecyl DPD which points to the importance of acyl tail length in HSL specificity. Three residues Asp73, Ser129, and, Trp 60 (Figure 2.7) seem to control alignment in the polar head cavity, while the hydrophobic tail sits in a very ordered hydrophobic pocket (Figure 2.8).

Table 2.1. Calculated Binding affinities using AutoDock Vina between LasR and the various forms of DPD, Pentyl- DPD and Dodecyl- DPD. (a. It has been noted that the difference between calculated binding energy and experimental value is ± 2.8 kcal/mol.⁶⁸)

AHL or analog	Binding Energy^a
3-oxo-dodecanoyl-HSL	-8.5 kcal/mol
Dodecyl DPD	
Dodecyl DPD - Cyclic	-7.8 Kcal/mol
Dodecyl DPD -Cyclic, hydrated	-7.8 Kcal/mol
Dodecyl DPD - Linear	-7.3 Kcal/mol
DPD	
DPD - Linear	-5.3 Kcal/mol
DPD - Cyclic	-5.6 Kcal/mol
DPD – Cyclic, hydrated	-5.3 Kcal/mol
Pentyl DPD	
Pentyl DPD - Linear	-6.4 Kcal/mol
Pentyl DPD – Cyclic	-6.8 Kcal/mol
Pentyl DPD – Cyclic, hydrated	-6.4 Kcal/mol

The alignment of DPD, pentyl DPD, and dodecyl DPD at the polar head (Figure 2.7) is vastly different. Even in the case of dodecyl DPD, where both computational analysis and biological assays confirm binding, there is rotation within the binding pocket. These results suggest a rather loose active site requirement in the polar head cavity.

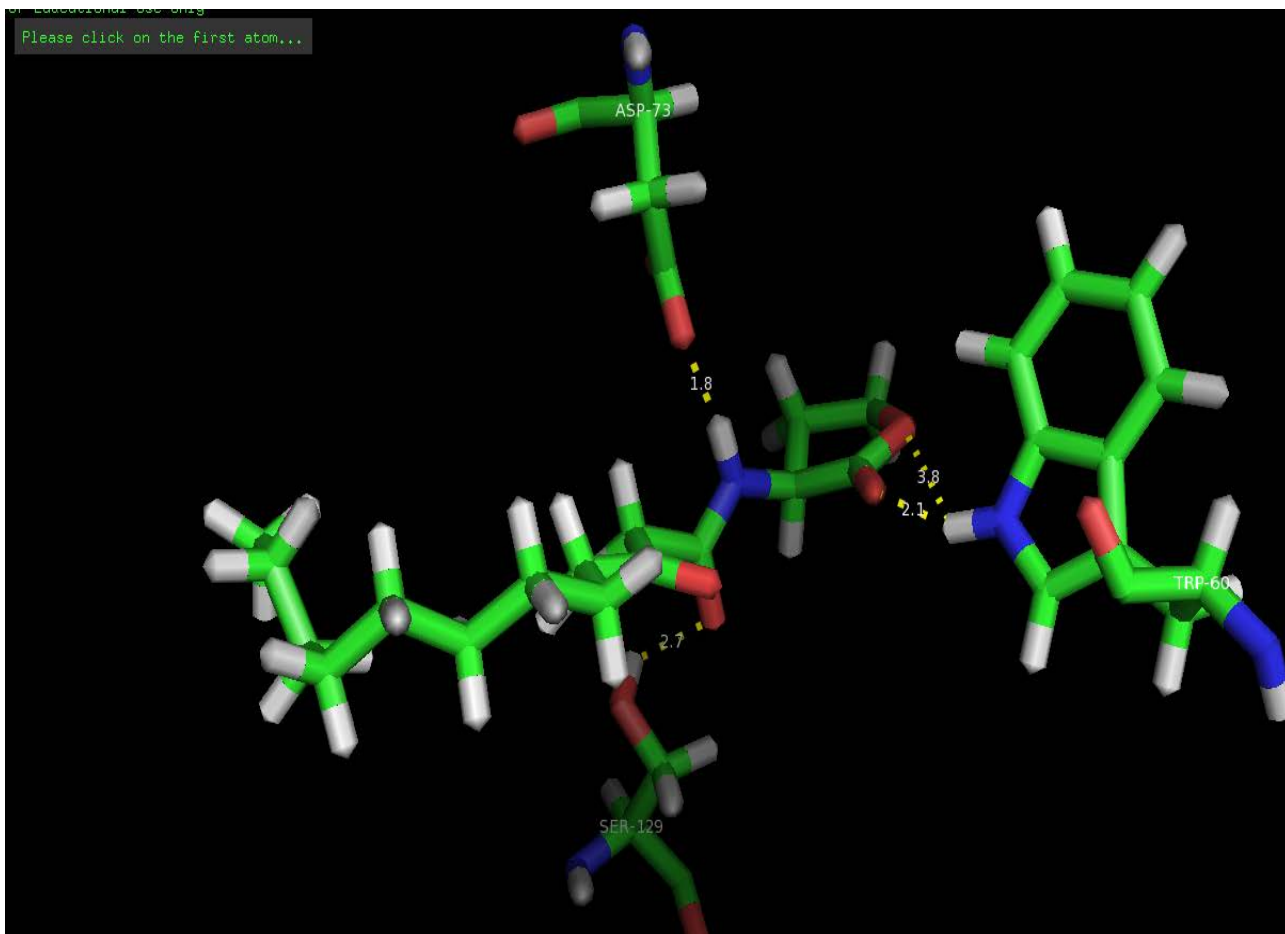


Figure 2.7 Hydrogen bond interactions involving 3-oxo-dodecanoyl in the LasR active site. The three catalytic residues are: Asp73, Ser129, Trp, 60.

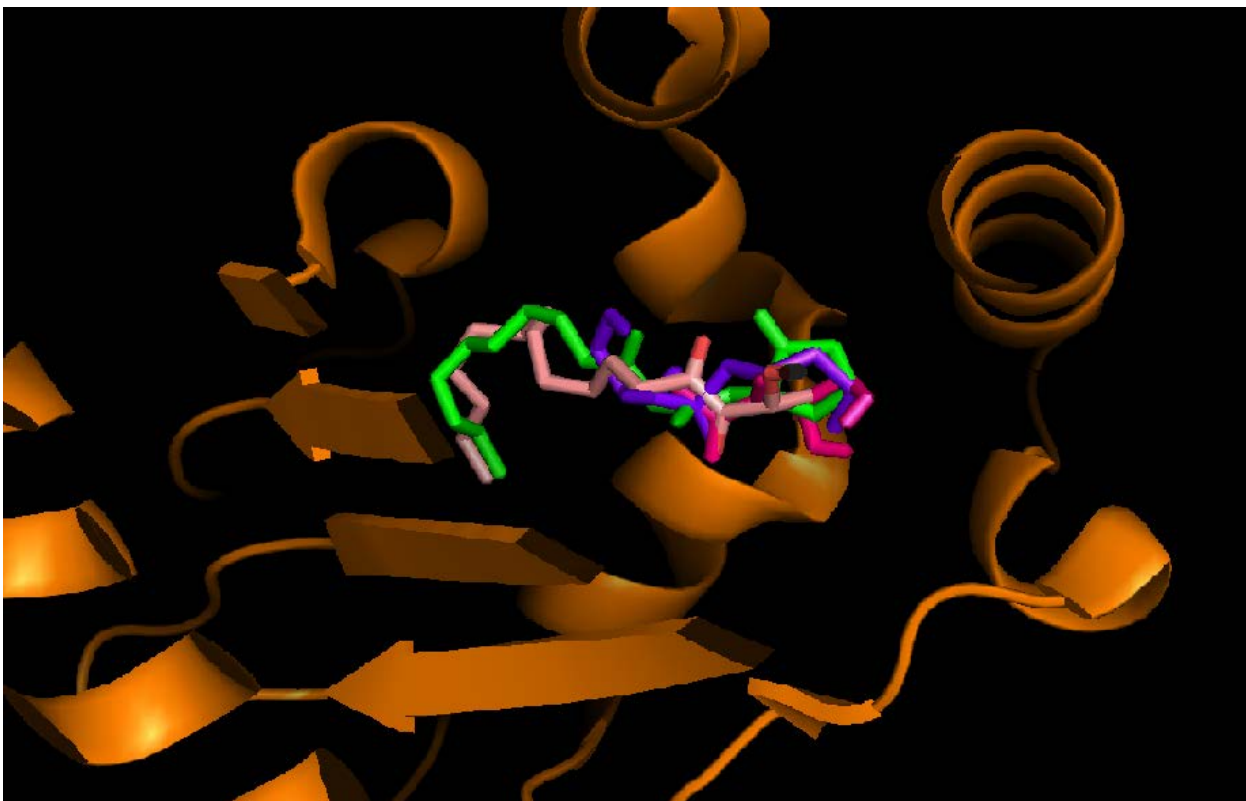


Figure 2.8. Superimposition of AI-2/analogs in the active site of LasR. Green- Native ligand, 3-oxo-decanoyl-HSL ; Pink – Dodecyl- DPD; Dark pink – DPD; Purple – Pentyl-DPD. All tabulated values correspond to an equivalent binding mode.

2.3 Preliminary results and future directions

As discussed previously, processing in enteric bacteria is dependent upon phosphorylation by LsrK. Likewise, all DPD analogs which can inhibit QS in *E.coli* and *S. typhimurium* are phosphorylated by LsrK. Antibiotics that depend on activation by bacterial enzymes can be rendered less effective by mutations. Thus, it was desirable to construct phosphorylated AI-2 analogs to eliminate the need for activation by the kinase, LsrK. However, the charged phosphate group generally imparts poor cellular permeability characteristics.

In addition, phosphate groups are rapidly cleaved by endogenous phosphatases, resulting in a significant and often total loss of activity. Broadly, there have been three types of phosphate isosteres that have been employed: (1) phosphorus based (2) carboxylate based (3) miscellaneous, non-phosphate based.⁶⁵ Thus, we envisioned synthesizing mimics of our phosphorylate compounds (Figure 2.9).

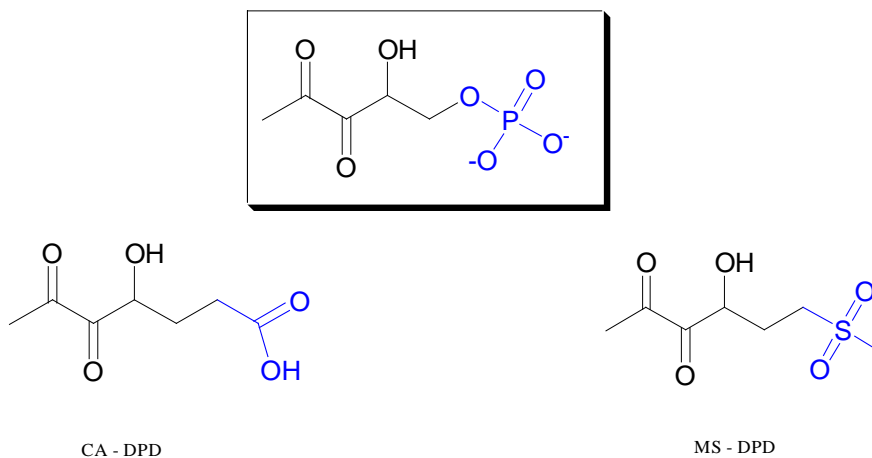
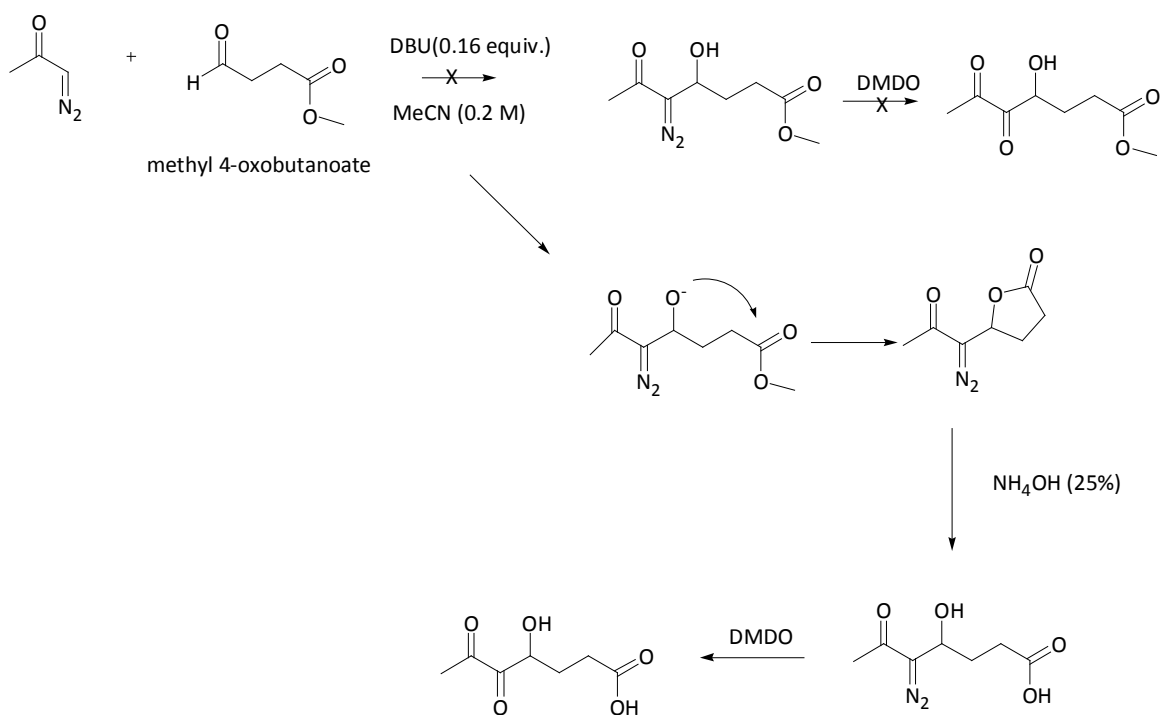


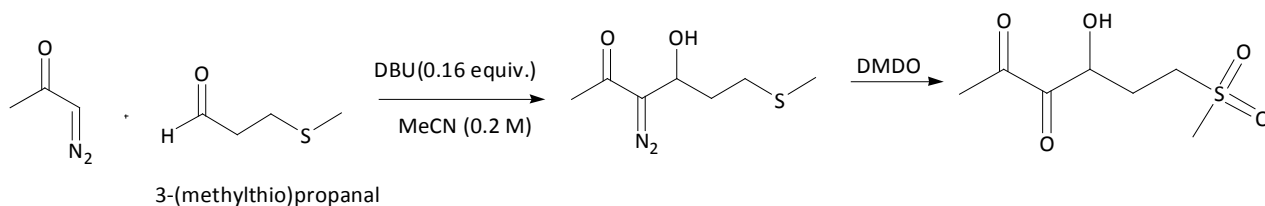
Figure 2.9. Structural relationship between phosphorylated DPD and phospho – mimics.

The first mimic we endeavored to make was a carboxylate derivative (Scheme 2.2). The synthesis utilized the familiar carbonyl condensation with the *t*-butylsiloxy acetaldehyde being replaced by methyl-4-oxobutanoate. NMR, IR, and MS confirmed that instead of the diazo carboxylate intermediate there was loss of methoxide consistent with the generation of the cyclic product. With this cyclic derivative in hand, it is expected that a basic workup (25% $\text{NH}_4\text{OH}/\text{H}_2\text{O}$) should yield the desired carboxylic acid DPD (CA-DPD).



Scheme 2.2 Synthesis of CA-DPD.

Next, we turned our attention to the synthesis of the sulfone mimic. The synthesis was identical to our general synthesis of AI-2 analogs, beginning with the addition of methyl diazocarbonyl to 3-(methylthio)-propenal (Scheme 2.3). Methyl sulfone DPD (MS DPD) was confirmed with ¹H NMR, ¹³C NMR, and ESI-MS (of the quinoxaline derivative, see supporting information).



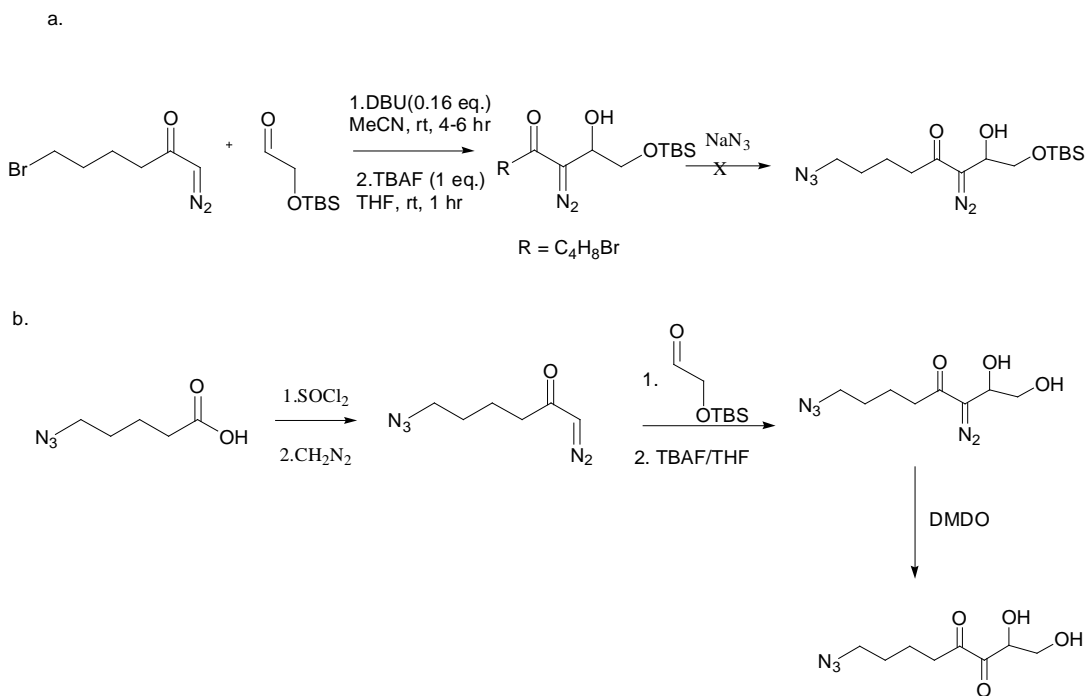
Scheme 2.3. Synthesis of MS – DPD

Future studies involving these phosphate mimics will focus on ascertaining the biological activity of these compounds. As these compounds are mimics of the native DPD molecule, they could activate QS in *E.coli* and *S.typhimurium*.

Alkyl-Azide DPD as a Chemical Probe

Quorum sensing is a rapidly evolving field, and, while there is a wealth of information including crystal structures and genomic analyses pertaining to AHL QS systems, AI-2 QS circuits are much more elusive. While we capitalize on the better known systems of *E. coli*, *S. typhimurium*, *P. aeruginosa*, and, *V. harveyi*, a chemical probe to identify putative AI-2 receptors in other bacteria would be invaluable to the field. Ideally, the probe would be a QS active molecule capable of forming a covalent linkage to AI-2 binding receptors *in vivo*. Azides are reactive molecules that are easily incorporated into molecules *via* the nucleophilic displacement of an alkyl halide. So, as our prototype of a molecular probe, we designed a C₄ azido DPD (C4A-DPD) (Scheme 2.4a). While the OTBS protected C₄Br diazo intermediate was confirmed with ¹H NMR, ¹³C NMR, MS and, IR, the displacement reaction failed to proceed.

The product could not be confirmed with NMR but, MS revealed a [M-28] ion consistent with the loss of N₂. This was puzzling as the reaction with the primary halide was expected to be facile.



Scheme 2.4. Synthesis of a reactive probe to detect QS receptors.

However, after multiple attempts, we abandoned our first approach towards azide DPD. Ultimately, the probe was constructed from the 5-azido pentanoic acid (Scheme 2.4b), once the acyl chloride was generated, the reaction proceeded according to our established synthesis.

Biological Evaluation of C₄-N₃ DPD in *E. coli* and *S. typhimurium*

β -Galactosidase activity (Figure 2.9) in the presence of 20 μ M AI-2 and 40 μ M C₄A-DPD was measured. The inhibition observed confirmed that this azido AI-2 analog is capable of antagonizing QS networks. Consequently, this enzyme must bind to LsrK and be phosphorylated. Based on previous studies, it appears that C₄A-DPD has an activity profile similar to that of pentyl DPD in *E. coli* and *S. typhimurium*. What is intriguing is the possibility of using C₄A-DPD to discover new QS regulatory proteins.

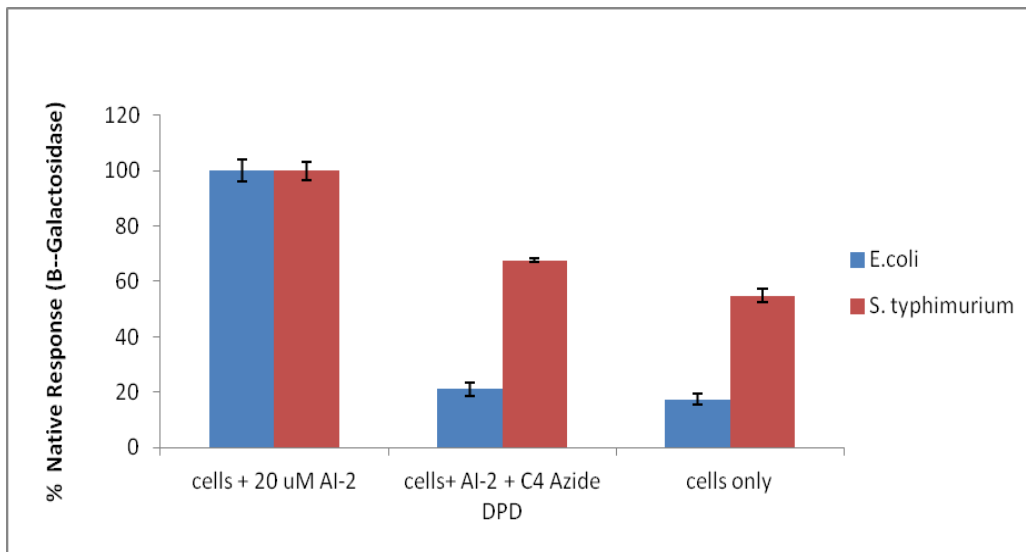


Figure 2.10. β -Galactosidase activity in response to the C₄ molecular probe (40 μ M).

Chapter Three

Discussion and Future Work

This work expands the utility of C₁ alkyl AI-2 analogs. In addition to serving as molecular probes in enteric bacteria such as *E.coli* and *S. typhimurium*, AI-2 analogs have been shown to be capable of attenuating QS in *P. aeruginosa*. Also, the effect of long chain AI-2 analogs on QS was found to be derived from a *specific* interception of the LasR receptor. Future work will be directed at the synthesis of more potent long chain C₁ AI-2 analogs. The design of these analogs will be governed by the results of computational studies with potential candidates. The main structural requirements of AI-1 analogs governed by the LasR active site are a polar head group combined with a hydrophobic region (Figure 3.1 A). Some logical alterations that could be made are increasing the number of polar groups and adding additional branching of the acyl tail (Figure 3.1 B). Additionally, the potency of AI-1 analogs is not only a function of their binding affinity to LasR but also their ability to permeate through cellular membranes. A long acyl tail, while important to LasR binding, would undoubtedly have problems crossing the lipophilic cell membrane. Future syntheses will involve the generation of structural mimics with more hydrophilic nature (Figure 3.1C).

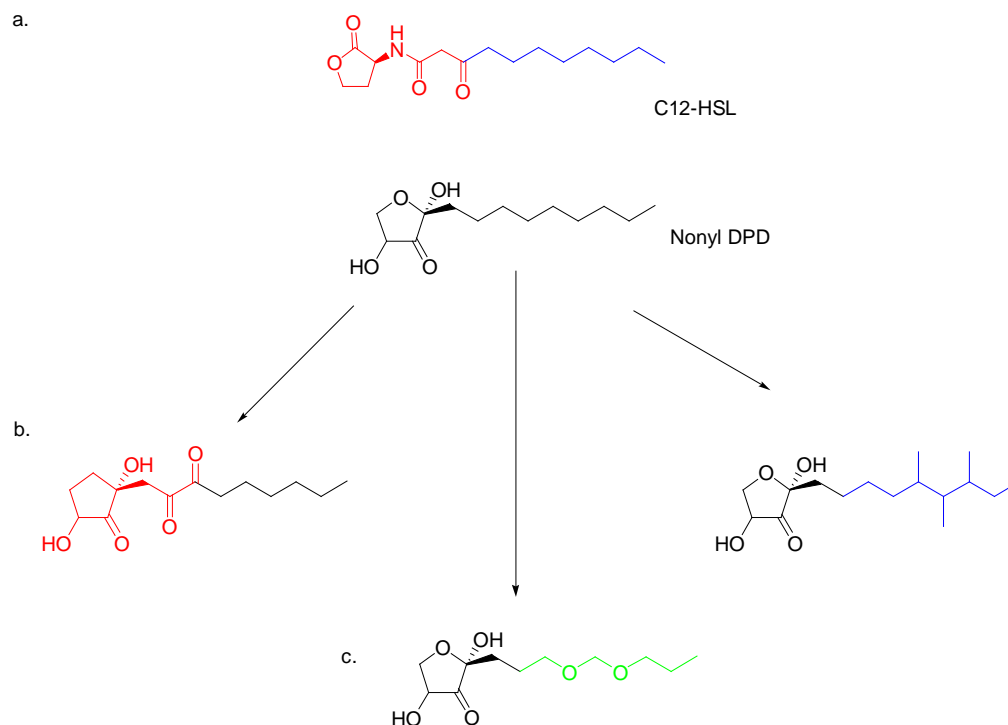


Figure 3.1. (a) Native AHL of *P. aeruginosa* (b) Structural changes in both the polar head region as well as the acyl tail for Nonyl- DPD (c) Introduction of more hydrophilic groups to enhance permeability.

The LasR receptor is typically responsive to AI-1 and analogs and this interaction between LasR and AI-2 analogs only underscores the utility of molecular probes. The first generation C4A-DPD described here will allow for the identification of novel AI-2 receptors across diverse bacterial species. This work also describes two novel C4 and C5 AI-2 analogs that will potentially allow for the development of more potent antagonists of AI-2. Eliminating the need for LsrK mediated phosphorylation of AI-2 analogs serves two purposes (1) more rapid delivery of antagonists to their cognate receptors and (2) avoids the possibility of analogs being rendered inactive by potential mutations in LsrK.

Future work with phospho-mimics will involve coupling the carboxylic acid or sulfone moiety to potent inhibitors such as isobutyl DPD, as we would expect additional enhancements in potency.

Lastly, work with *bis*-ester protected AI-2 analogs highlights the importance of using probes to understand QS processing. From these studies it is clear that different protection strategies may be necessary for specific bacteria. For example, *E.coli* is generally responsive to *bis* protected esters while *S. typhimurium* is not.

Chapter Four

Materials and Methods, Supplemental Figures, References

4.1 General Methods

Moisture sensitive reactions were carried out using oven dried glassware sealed with rubber septa under argon. Dry MeCN was distilled over CaH₂ immediately prior to use. Dry THF was purchased from Sigma Aldrich and used without further distillation. All organic solutions were concentrated using a Buchi rotary evaporator with an aspirator pump. Thin-layer chromatography was conducted with Merck Kieselgel 60 F254 plates. TLC plates were visualized with UV light and *p*-anisaldehyde stain. Crude reaction mixtures were purified by flash chromatography using 230-400 mesh silica gel.

¹H NMR and ¹³C NMR were measured with Bruker AV-400 at 400 MHz and 100 MHz respectively. Data for ¹H NMR were reported according to standard convention as follows: chemical shift (ppm; s = singlet, d = doublet; t = triplet; q = quartet, dd = doublet of doublet; td = triple of doublets; m = multiplet), coupling constant (Hz), and integration. Data for ¹³C NMR are reported in terms of chemical shift (ppm) relative to solvent peak. Mass spectra and high resolution mass spectra were recorded by JEOL AccuTOF-CS (ESI positive/ ESI negative (as indicated), needle voltage 1800-2400 eV). IR spectra were measured with a ThermoNicolet (IR200) spectrophotometer.

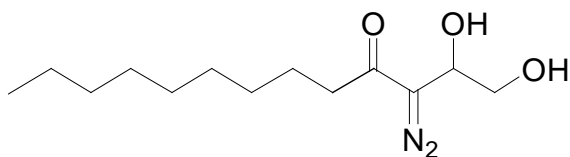
Generation of Acyldiazomethane and Diazocarbonyls: Acyldiazomethane was generated from the base, NaOH (8g, 0.35 mol) catalyzed hydrolysis of Diazald (10g, 24.6 mmol) (SigmaAldrich) in ethanol and water (1:1, 20 mL) at 75 °C. Acyldiazomethane was removed under vacuum as an acetone solution at -70 °C. The diazocarbonyls were synthesized from the addition of the requisite acyl chlorides (1 equiv.) and acyldiazomethane (3 equiv.) at 0 °C for 2 hr.

Synthesis of Diazodiols: 2-(*t*-butyldimethylsiloxy) acetaldehyde (1.1 equiv.) was added to a solution of diazocarbonyl (0.2M) and DBU (0.16 equiv.) in anhydrous acetonitrile at RT. The reaction was performed under argon and monitored by TLC. The reaction was quenched after 8 h with satd. NaHCO₃, extracted with dichloromethane (3 x 15 mL), and dried over sodium sulfate. The solvent was evaporated and the crude residue was redissolved in anhydrous THF (0.2M). To this solution was added TBAF (1equiv.). The solution was allowed to warm to room temperature for 1 h. The solvent was removed under reduced pressure and the crude product was purified by column chromatography. The product eluted as a bright yellow oil with 1:3 to 3:2 ethyl acetate: hexane (45 – 60% yield).

Synthesis of DPDs: To a solution of diazodiol (5 mg) in acetone (1mL) was added dimethyldioxirane (1mL). The reaction was stirred at room temperature until the disappearance of starting material as monitored by IR (loss of sharp stretch at 2080 cm⁻¹). Solvent and excess dioxirane was removed under reduced pressure; NMR was taken without further purification.

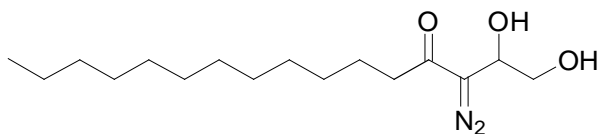
Synthesis of Quinoxaline Derivatives: To a solution of DPD was added 1,2-phenyldiamine (2 equiv.) , the reaction mixture was stirred for 24 hrs, after which, the reaction was quenched with 1 M HCl. The quinoxaline was extracted with chloroform, the solvent removed under pressure, and the crude product purified on silica.

4.2 Spectroscopic Characterizations



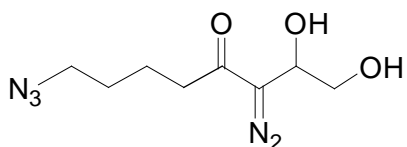
3-Diazo-1,2-dihydroxy-tridecan-4-one:

^1H NMR (400 MHz, CDCl_3) δ 4.78 (t, $J = 4.6$ Hz, 1H), 3.89 (dd, $J = 11.5, 4.3$ Hz, 1H), 3.79 (dd, $J = 11.5, 4.9$ Hz, 1H), 2.58 – 2.45 (m, 2H), 1.66 (m, 2H), 1.43 – 1.21 (m, 14H), 0.91 (t, $J = 6.7$ Hz, 3H). ^{13}C NMR (100 MHz, CDCl_3 , δ): 14.5, 15.7, 23.1, 29.5, 29.6, 29.7, 29.7, 32.3, 38.7, 66.3, 67.2. IR (cm^{-1} , CHCl_3): 3421.2, 2926.4, 2854.3 , 2087.1 , 1621.7.



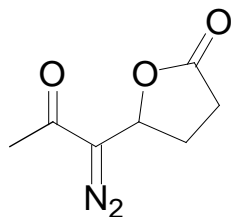
3-Diazo-1,2-dihydroxy-hexadecan-4-one:

^1H NMR (400 MHz, CDCl_3) δ 4.78 (t, $J = 4.6$ Hz, 1H), 3.88 (dd, $J = 11.9, 3.9$ Hz, 1H), 3.82 – 3.73 (m, 1H), 3.55 – 3.46 (m, 1H), 2.74 (s, 1H), 2.57 – 2.44 (m, 2H), 1.75 – 1.61 (m, 4H), 1.41 – 1.26 (m, 16H), 0.96 – 0.84 (m, 3H) ^{13}C NMR (100 MHz, CDCl_3 , δ): 14.5, 23.1, 25.0, 29.6, 29.7, 29.8, 29.9, 30.0, 30.0, 30.1, 32.3, 38.7, 64.7, 67.1, 195.6. IR (cm^{-1} , CHCl_3): 3362.9, 2920.9, 2851.9, 2083.6, 1612.7.



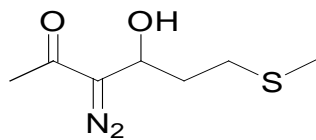
8-Azido-3-diazo-1,2-dihydroxy-octan-4-one:

^1H NMR (400 MHz, CDCl_3) δ 4.18 – 4.05 (m, 1H), 3.83 (dt, $J = 9.9, 4.7$ Hz, 1H), 3.73 (d, $J = 9.9$ Hz, 1H), 3.32 (t, $J = 6.5$ Hz, 2H), 2.33 (t, $J = 7.2$ Hz, 2H), 1.80 – 1.59 (m, 4H)
 ^{13}C NMR (100 MHz, CDCl_3) δ 22.6, 28.7, 37.8, 51.5, 64.8, 66.5, 96.3, 198.5. IR (cm^{-1} , CHCl_3): 3374.8, 2922.3, 2359.1, 2083.3, 1608.01.



5-(1-Diazo-2-oxo-propyl)-dihydro-furan-2-one:

^1H NMR (400 MHz, CDCl_3 , δ): δ 5.59 – 5.50 (m, 1H), 2.80 – 2.54 (m, 2H), 2.31 (s, 3H), 2.25 – 2.06 (m, 2H). ^{13}C NMR (100 MHz, CDCl_3) δ 26.3, 26.7, 29.3, 74.1, 177.0. IR (cm^{-1} , CHCl_3): 3000-2900, 2090.7, 1771.8, 1642.7.

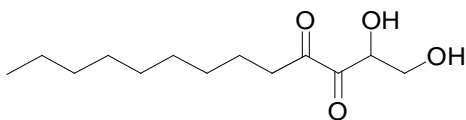


3-Diazo-4-hydroxy-6-methanesulfanyl-hexan-2-one:

^1H NMR (400 MHz, CDCl_3) δ 4.95-4.92(m,1H), 2.68-2.66 (m, 2H), 2.28 (s, 2H), 2.14 (s, 1H), 1.99-1.86(m, 2H). ^{13}C NMR (100 MHz, CDCl_3) δ 15.9, 26.2, 30.6, 33.5, 65.4, 191.9. IR (cm^{-1} , CHCl_3): 3387.9, 2918.3, 2084.5, 1715, 1614.50.

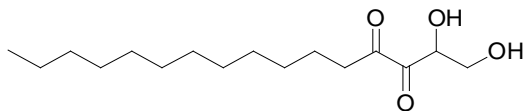
DPD derivatives:

As discussed previously. DPD derivatives are a mixture of interconverting structures and are ultimately confirmed *via* their quinoxaline derivatives. See supplementary figures below.



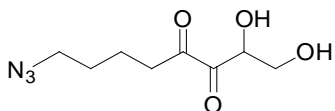
1,2-Dihydroxy-tridecane-3,4-dione

^1H NMR (400 MHz, MeOD) δ 4.11-4.05(m), 3.90-3.83(m), 3.78-3.71(m), 2.83-2.63(m), 1.60-1.35(m), 0.89 (s). ^{13}C NMR (100 MHz, MeOD) δ 32.1, 29.7, 28.9, 22.7, 13.3. IR (cm^{-1} , MeOD): 3421.2, 2926.4, 2854.3, 1621.7



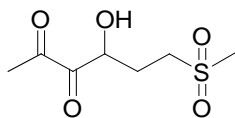
1,2-Dihydroxy-hexadecane-3,4-dione

^1H NMR (400 MHz, MeOD) δ 4.28-4.12(m), 4.01-3.87(m), 3.71-3.58(m), 3.47-3.36(m), 2.50-2.37(m), 2.27-2.09(m), 1.99-1.92(m), 1.35-1.16(m), 1.00-0.80(m), 0.53-0.42(m). ^{13}C NMR (100 MHz, MeOD) δ 32.3, 30.1, 29.8, 23.1, 14.6. IR (cm^{-1} , CHCl_3): 3362.9, 2920.9, 2851.9, 1612.7.



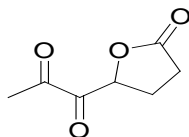
8-Azido-1,2-dihydroxy-octane-3,4-dione

^1H NMR (400 MHz, MeOD) δ 4.05, 3.29, 2.73, 2.23, 1.60, 1.27, 0.82. ^{13}C NMR (100 MHz, MeOD) δ 74.3, 62.4, 51.5, 36.5, 33.3, 29.3, 28.4, 22.2, 20.4, 20.1. IR (cm^{-1} , MeOD): 3374.8, 2922.3, 2359.1, 1608.01.



4-Hydroxy-6-methanesulfonyl-hexane-2,3-dione

^1H NMR (400 MHz, MeOD) δ 3.22, 2.56, 2.07, 1.95, 1.50. ^{13}C NMR (100 MHz, MeOD) δ 207.9, 72.1, 51.4, 50.2, 39.9, 23.9. IR (cm^{-1} , MeOD): 3387.9, 2918.3, 1715, 1614.50



1-(5-Oxo-tetrahydro-furan-2-yl)-propane-1,2-dione

^1H NMR (400 MHz, MeOD) δ 2.76, 2.51-2.49(m), 2.25-2.09(m), 1.65-1.47(m). ^{13}C NMR (100 MHz, MeOD) δ 206.1, 178.7, 99.7, 81.9, 80.8, 27.5, 26.2, 23.7, 21.9, 21.1. IR (cm^{-1} , CHCl_3): 3000-2900, 1771.8, 1642.7.

4.3 Methods of Biological Evaluation

Bacterial Strains and Growth Conditions: *P. aeruginosa* bioluminescent reporter

(LasR:LasI:LuxCDABE) strains⁶⁶ were cultured in Luria Bertani medium (LB, SigmaAldrich) at 37 °C with 200 $\mu\text{g}/\text{mL}$ ampicilin. *S. typhimurium* and *E. coli* β -galactosidase expressing reporter strains (Lsr:LacZ) were cultured in LB media at and 37 °C with the appropriate antibiotics (100 $\mu\text{g}/\text{mL}^{-1}$ kanamycin, and 50 $\mu\text{g}/\text{mL}$ ampicilin, respectively).

Measurement of the QS Response in P. aeruginosa: Compounds were measured for their ability to induce (QS agonists) or inhibit (QS antagonists) bioluminescence in PSB1075. *P. aeruginosa* was grown for 18 hrs. at 37°C in LB media and diluted 1:100 into fresh LB media.

P. aeruginosa was grown for an additional 3-4 hours (OD = 0.4) and diluted once again (1: 50 into fresh LB media), and grown for an additional 30 minutes. 1 mL of this culture was diluted into 9 mL fresh LB and, this resultant mixture was inoculum

Agonistic Assays:

200 µL of inoculum was added to 96 well plates and aliquots of the native HSL or analogs (40 µM) were added directly. The plate was covered and allowed to incubate at 37 °C for 8 hours. OD₆₀₀ (as a measure of growth) was measured in a side by side experiment with 500uL of inoculum. Bioluminescence was recorded every hour.

Induction of luminescence indicated the ability of HSL or analog to activate QS. All experiments were done in triplicate and repeated at least twice. Error bars represent the standard deviation.

Antagonistic Assays:

Before antagonistic assays were performed, IC₅₀ experiments were carried out to determine concentrations of HSL needed to induce significant bioluminescence in PSB1075.

200 µL of inoculum was added to 96 well plates, followed by the addition of 20 µM HSL, and, the subsequent addition of 40 µM analog. Bioluminescence was recorded every hour. Reduction of luminescence indicated the ability of HSL or analog to inhibit QS.

Negative Control: Constitutive Reporter

P. aeruginosa MET2442 was cultured in the same manner as PSB1075. Experiments with this strain were similar to those of the agonistic assay. MET2442 was constructed with a mini-transposon (LuxCDABE) and thus was expected to exhibit the same level of bioluminescence regardless of the compounds it was cultured with.

Measurement of the QS Response in S. typhimurium and E. coli: Compounds were measured for their ability to induce (QS agonists) or inhibit (QS antagonists) β -galactosidase expression. β -galactosidase expression was determined by incubation with the substrate *O*-nitrophenyl- β -D-galactoside and release of *O*-nitrophenyl (420 nM) indicated the activity of β -galactosidase. *S. typhimurium* (MET715) and *E. coli* (LW7) were grown for 18 hrs in LB media.

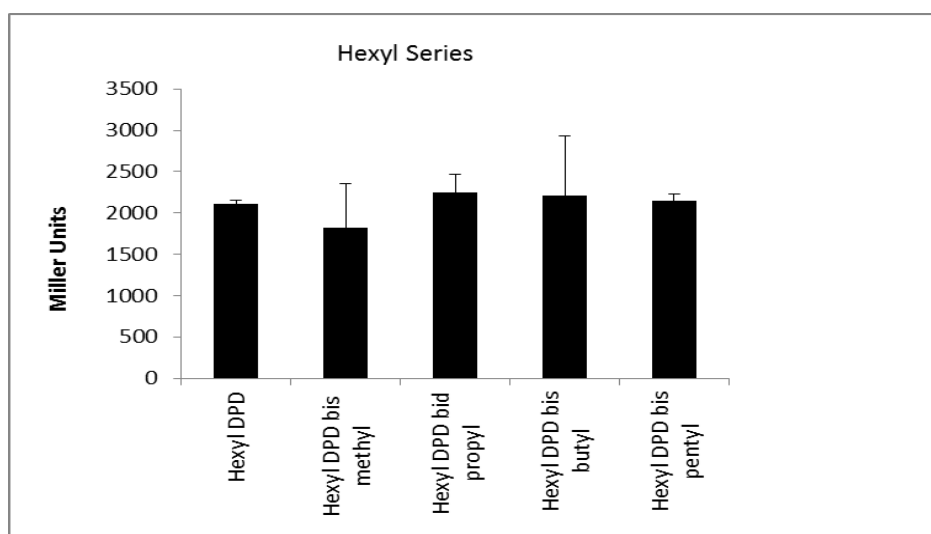
Cultures were diluted (1:50 in fresh LB with appropriate antibiotics) and scaled up for an additional 4 hours (OD = 0.5-1.0). Cells were harvested by centrifugation at 14K rpm for 10 minutes and resuspended in an equal volume of PBS buffer.

Suspensions of either *S. typhimurium* or *E. coli* were cultured with 40 μ M analog (agonistic response) or both analog and 20 μ M AI-2 (antagonistic response) for 2hrs. AI-2 dependent β -galactosidase production was quantified by the Miller assay.⁶⁷

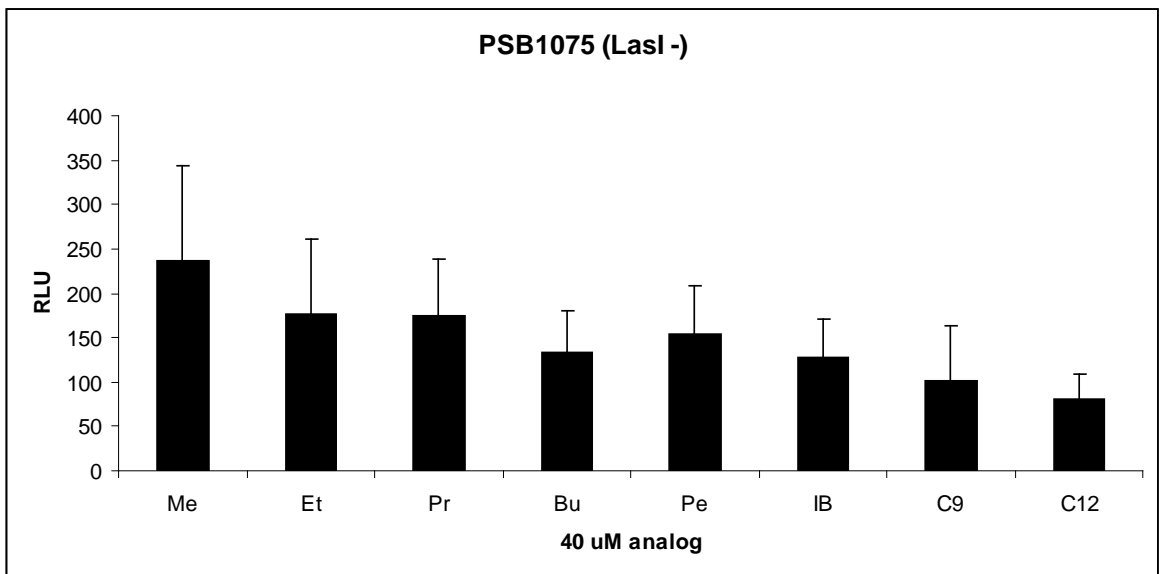
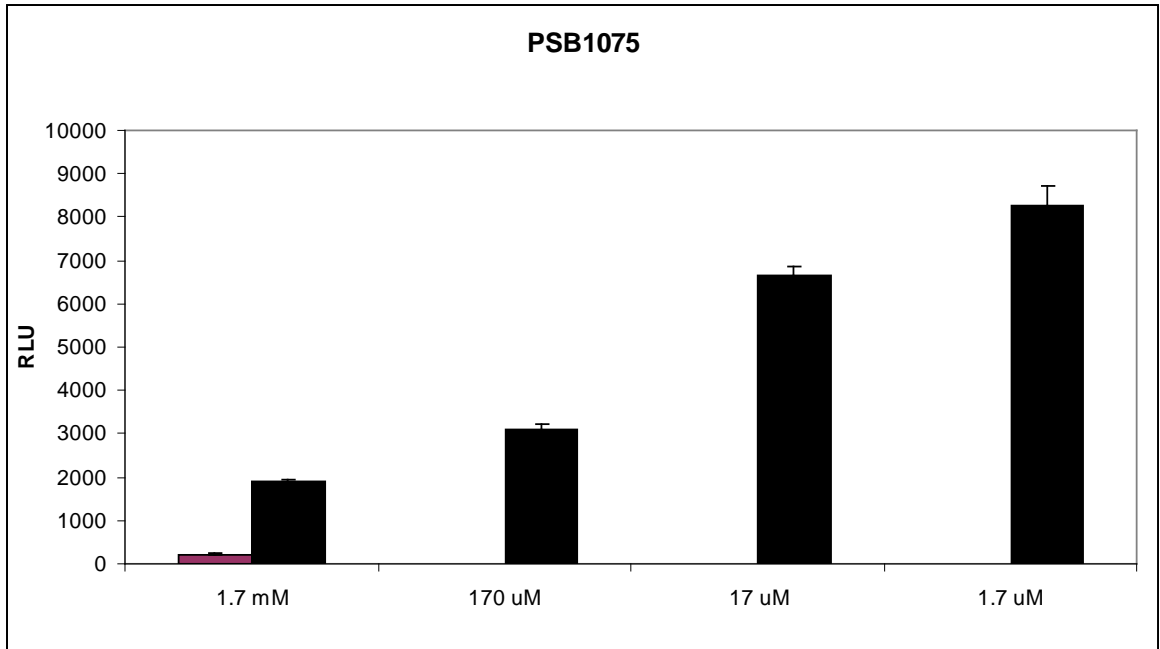
4.4 Computational Analysis of LasR Binding Pocket

AutoDock Vina⁶⁸ was used to model binding interactions between LasR and its native HSL as well as AI-2 analogs in their various forms. 3-oxo-decanoyl-HSL was used as a control to ensure that analogous binding modes were being compared. Once, the native ligand was successfully docked in the binding pocket with a high affinity, binding affinities (kcal mol⁻¹) for the various AI-2 analogs were computed.

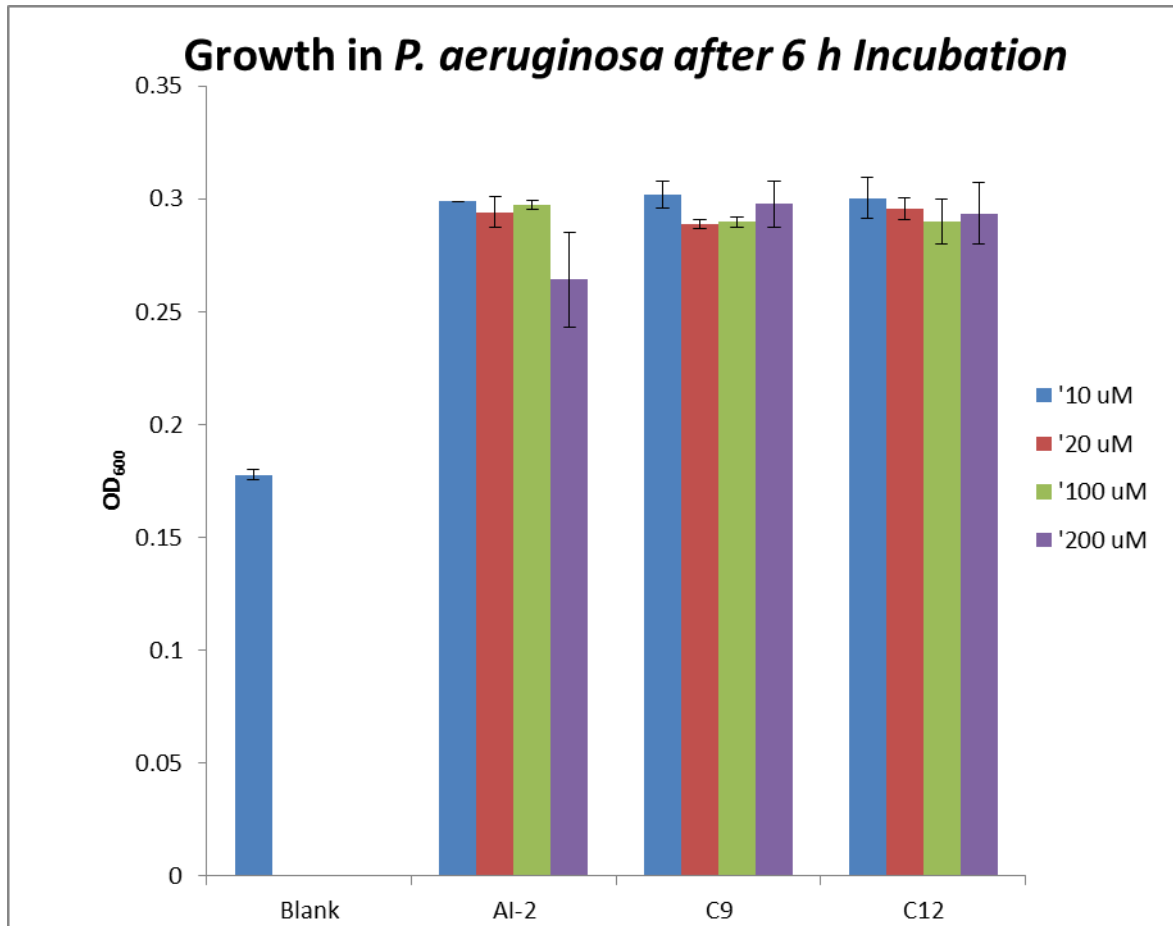
4.5 Supplementary Figures



S1. QS response in *S.typhimurium* in response to *bis* ester protected hexyl analogs (20 μ M) and AI-2 (20 μ M).



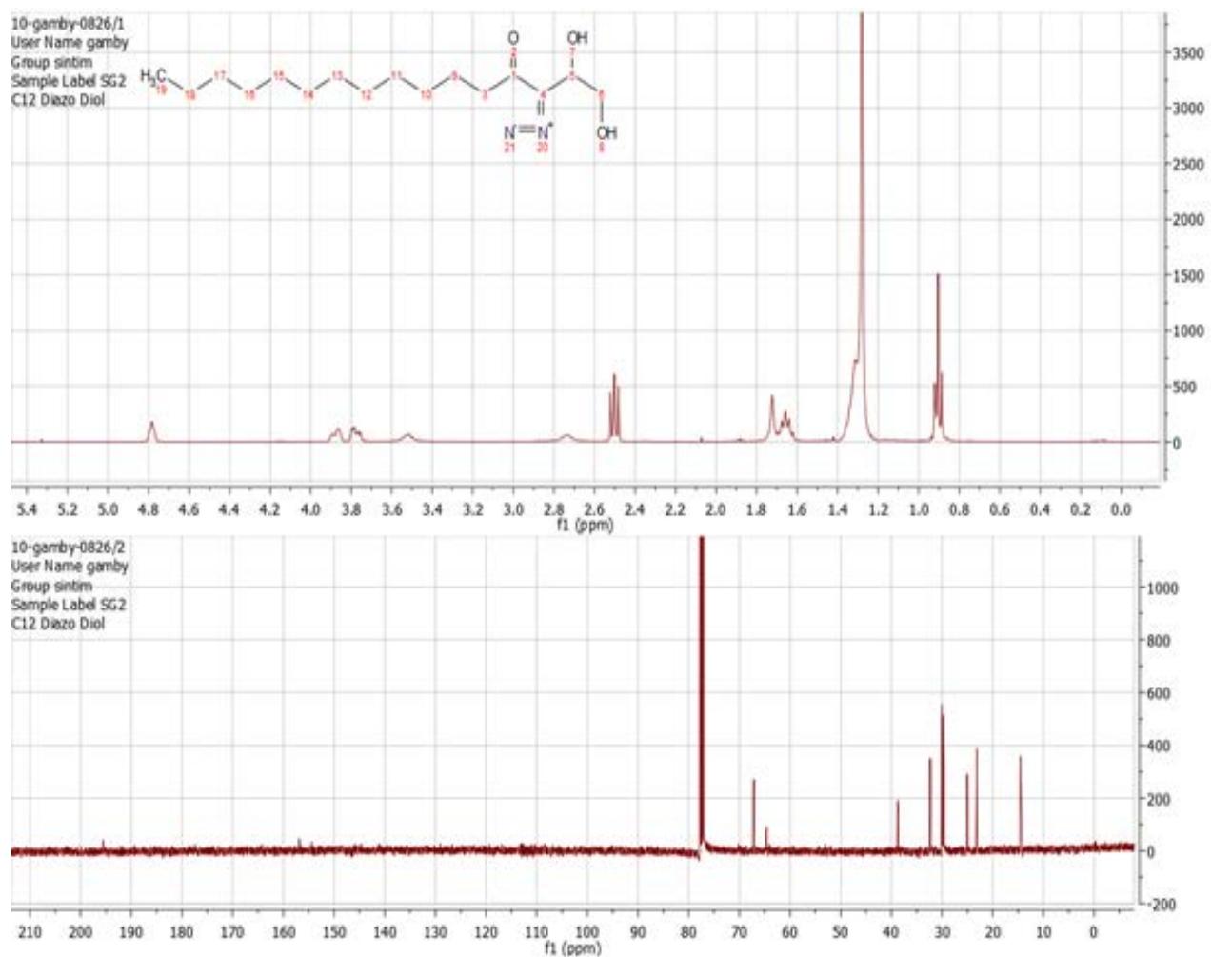
S2. (Top) Induction of QS in *P.aeruginosa* in response to the native HSL. (Bottom) AI-2 analogs do not induce a QS response in *P.aeruginosa*.



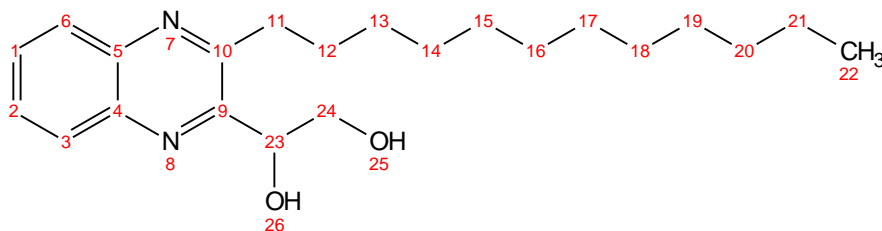
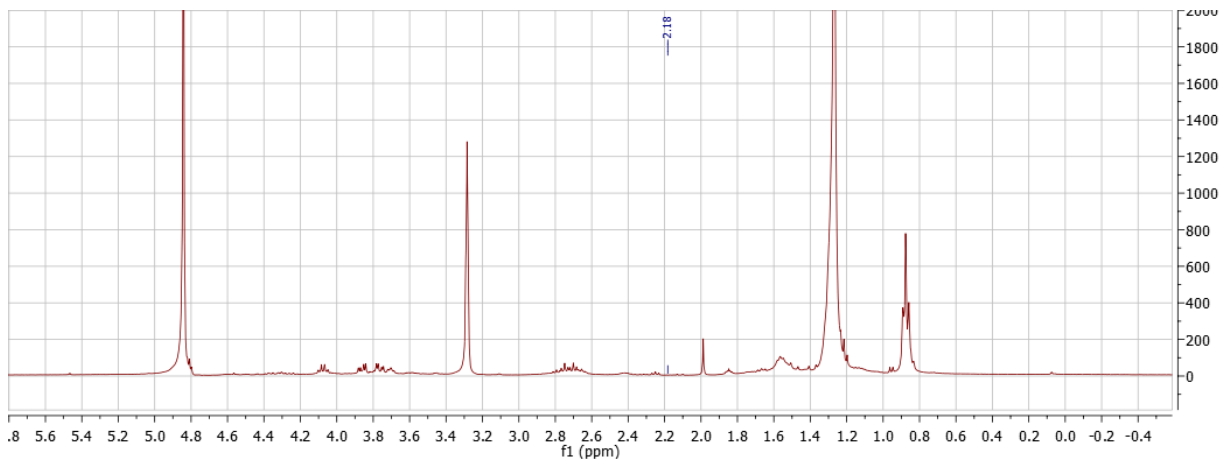
S3. Growth determinations in response to varying concentrations of methyl, nonyl, and dodecyl DPD.

Spectral Characterizations:

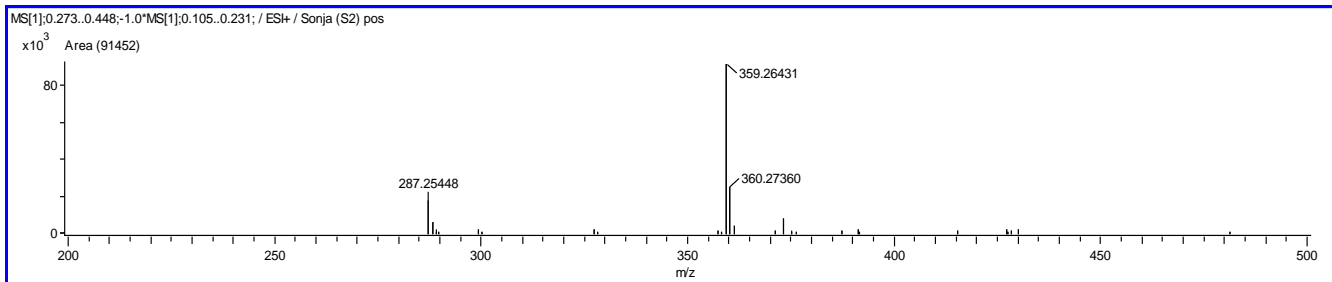
C12 Diazo Diol (^1H NMR, ^{13}C NMR)



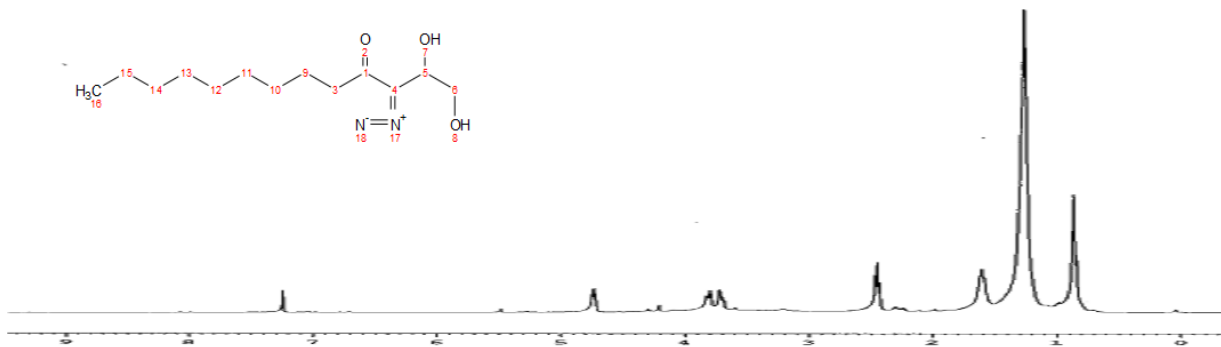
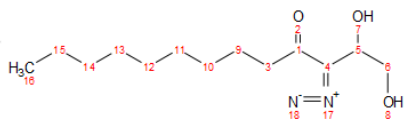
C12 DPD (Top) → Quinoxaline derivatization with phenylenediamine (Bottom)



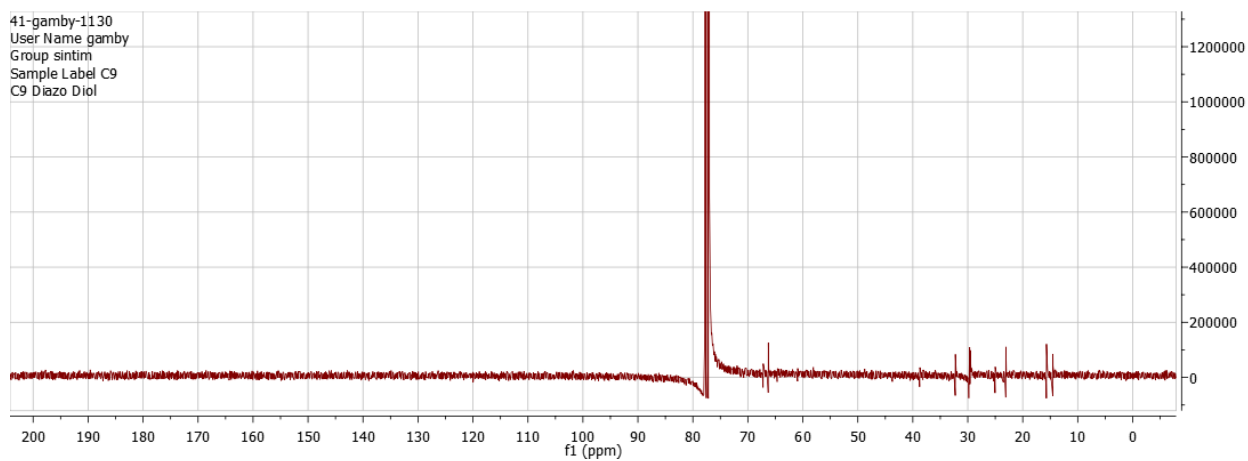
[M+H]⁺ (expected) = 359.26980
(actual) = 359.26431



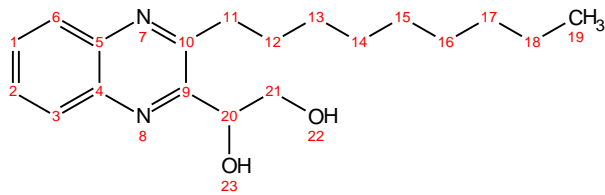
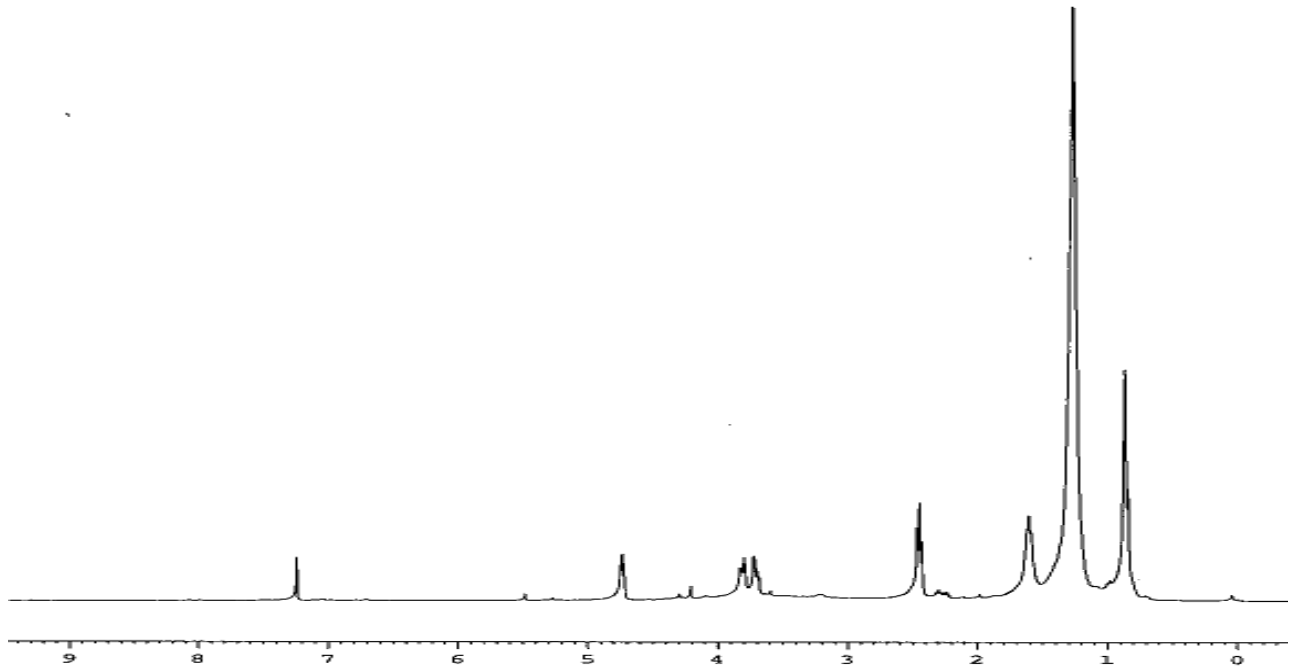
C9 Diazo Diol (¹H NMR, ¹³C NMR)



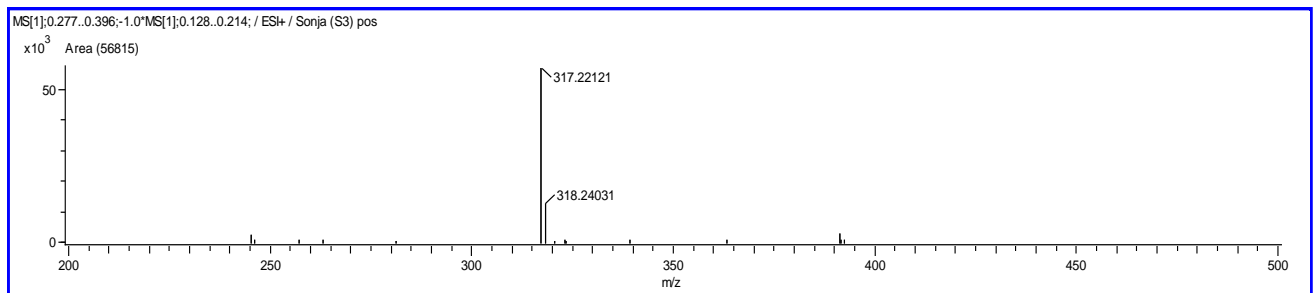
41-gamby-1130
User Name gamby
Group sintim
Sample Label C9
C9 Diazo Diol



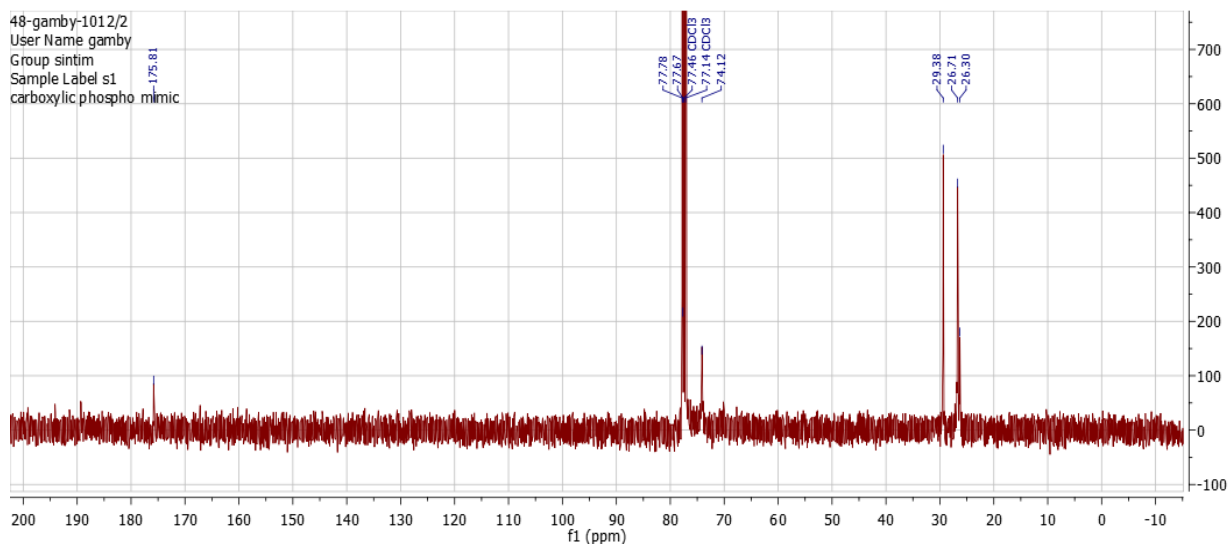
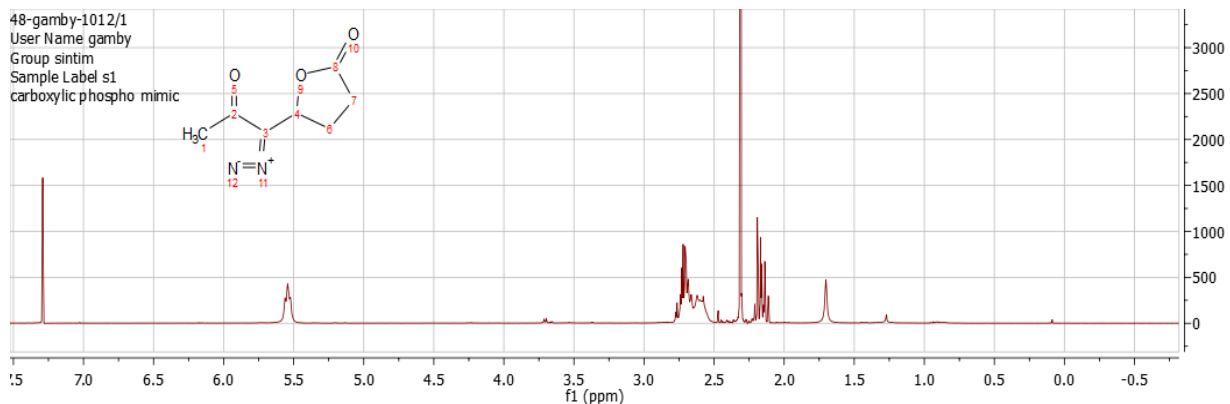
C9 DPD (Top) → Quinoxaline derivatization with phenylenediamine (Bottom)



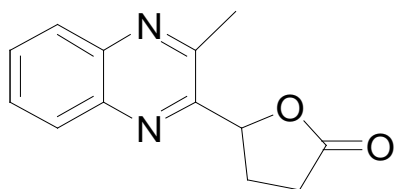
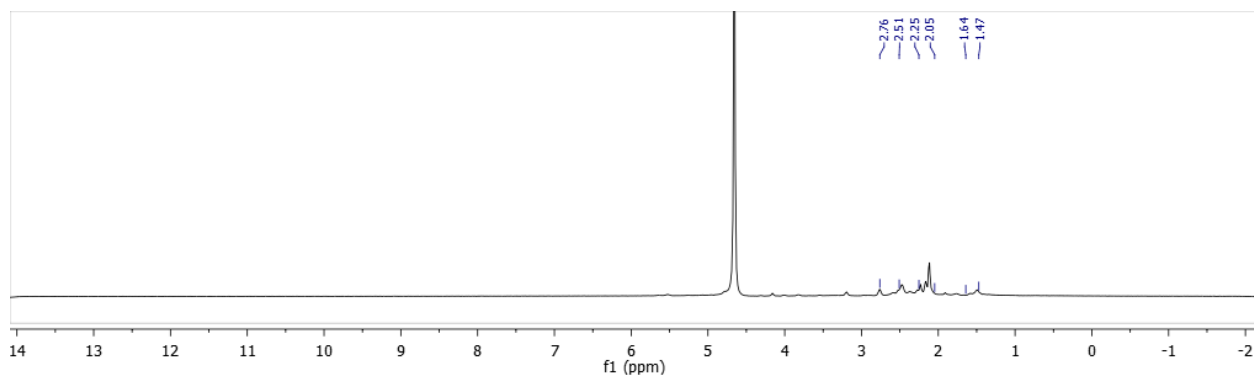
$[M+H]^+$ (expected) = 317.22290
(actual) = 317.22121



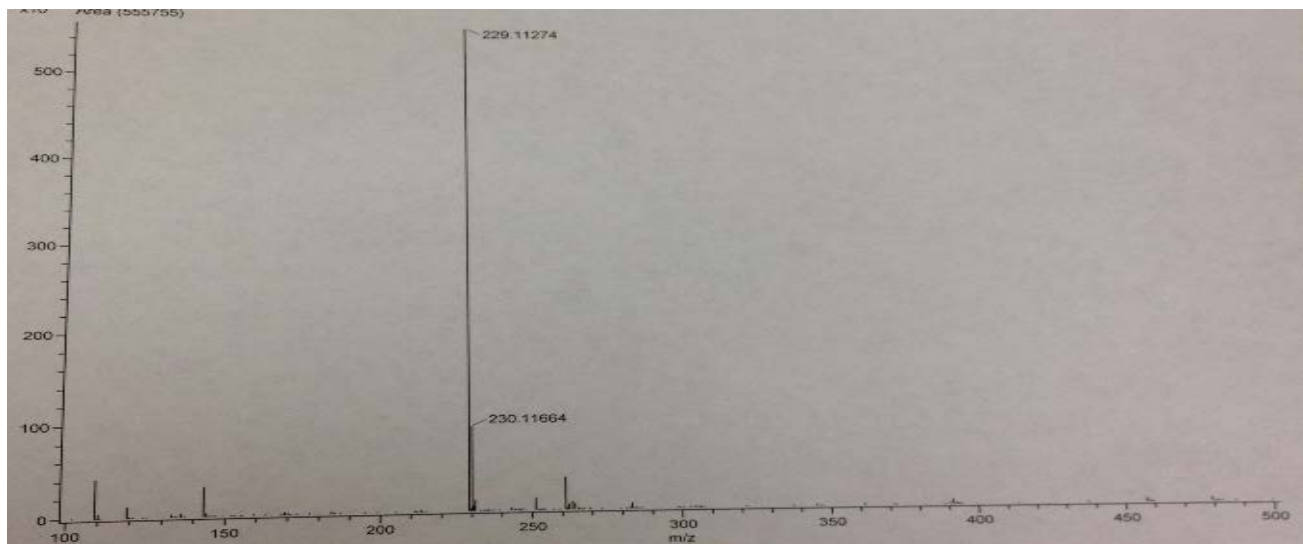
CA Diazo Diol (¹H NMR, ¹³C NMR)



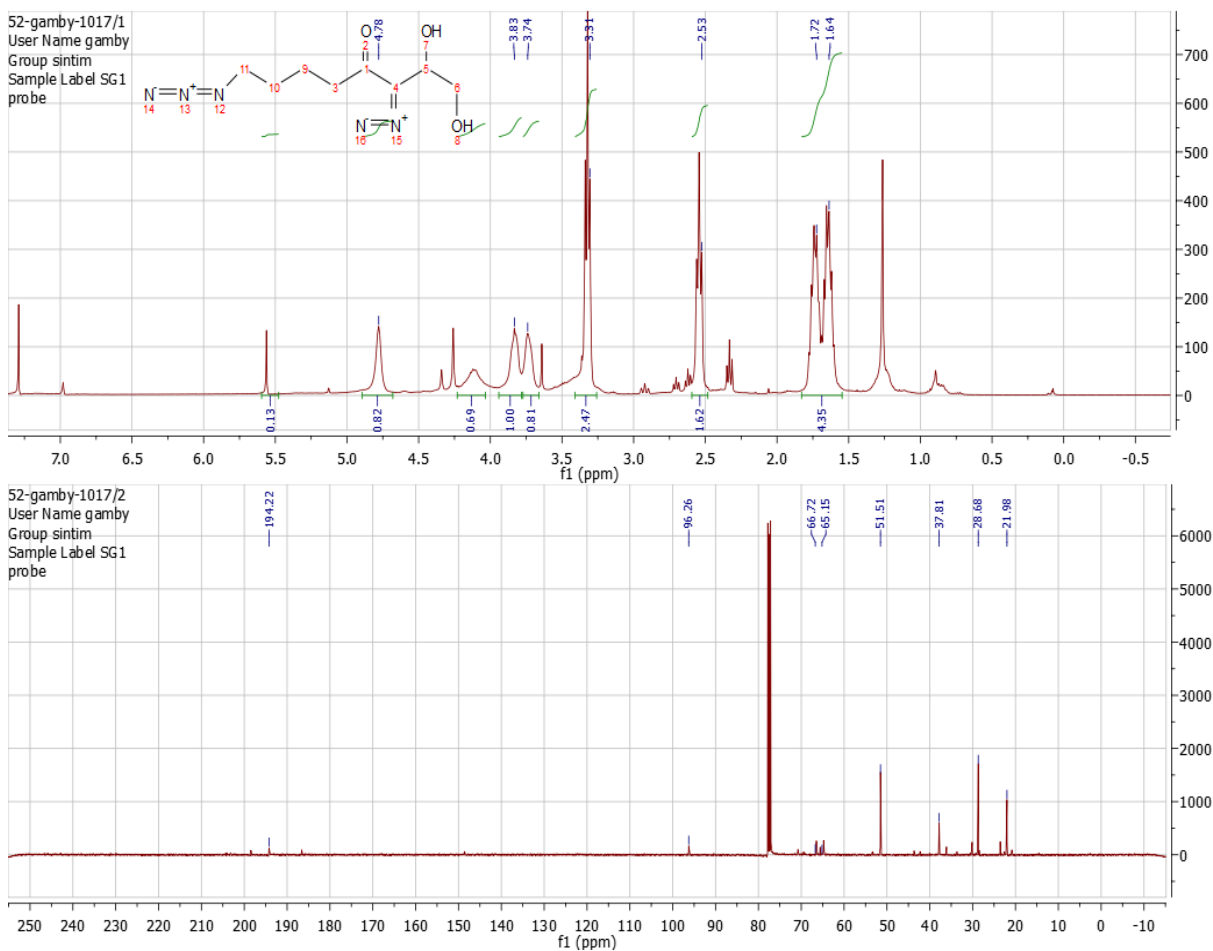
CA DPD (Top) → Quinoxaline derivatization with phenylenediamine (Bottom)



[M+H]⁺ (expected): 229.0977
(actual): 229.11274

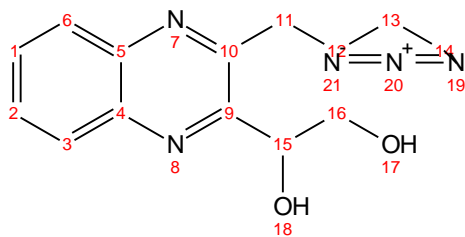
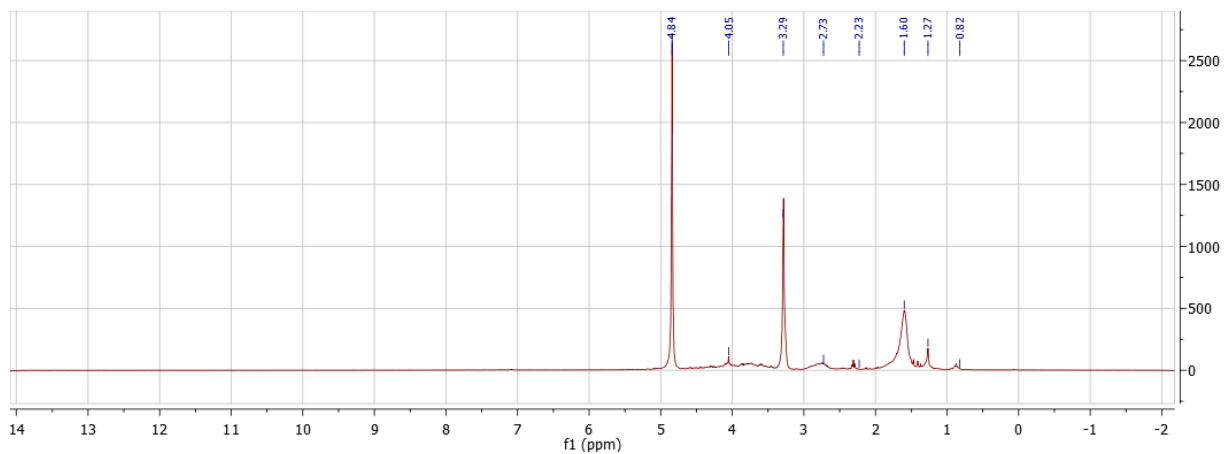


C4 Azide Diazo Diol (¹H NMR, ¹³C NMR)



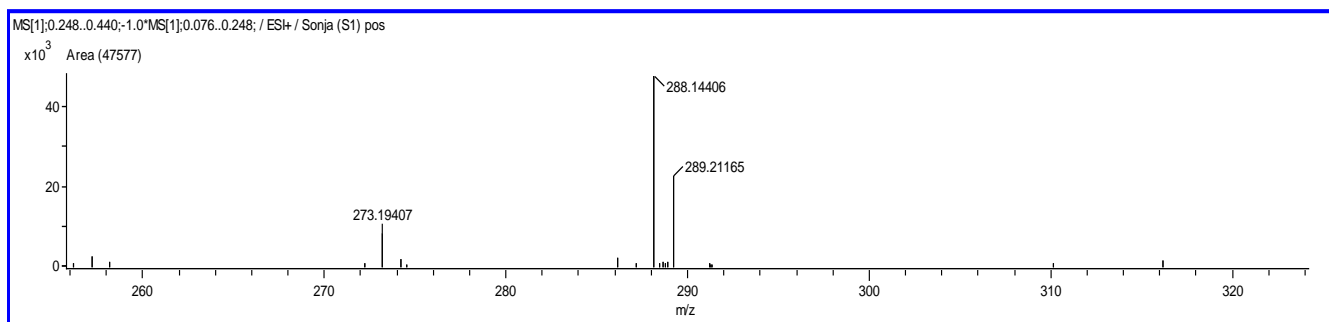
C4 Azide DPD (Top) → Quinoxaline derivatization with phenylenediamine

(Bottom)

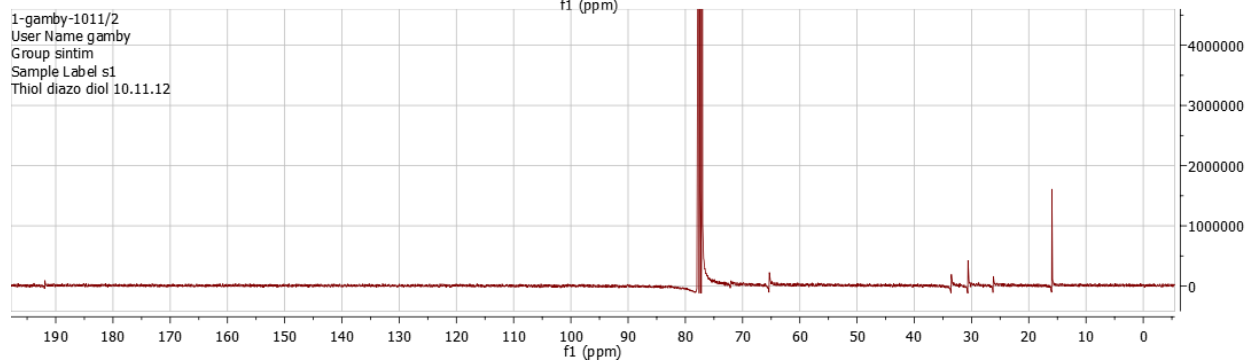
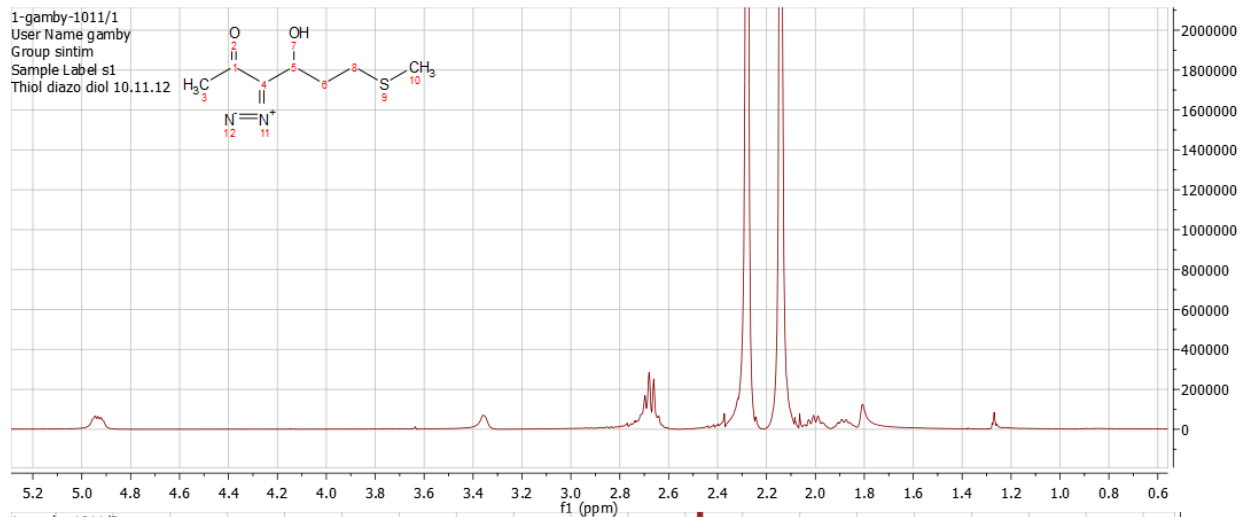


$[M+H]^+$ (expected) = 288.1460

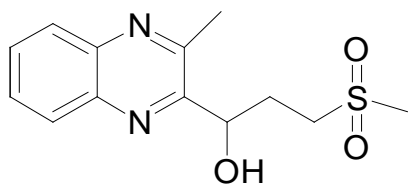
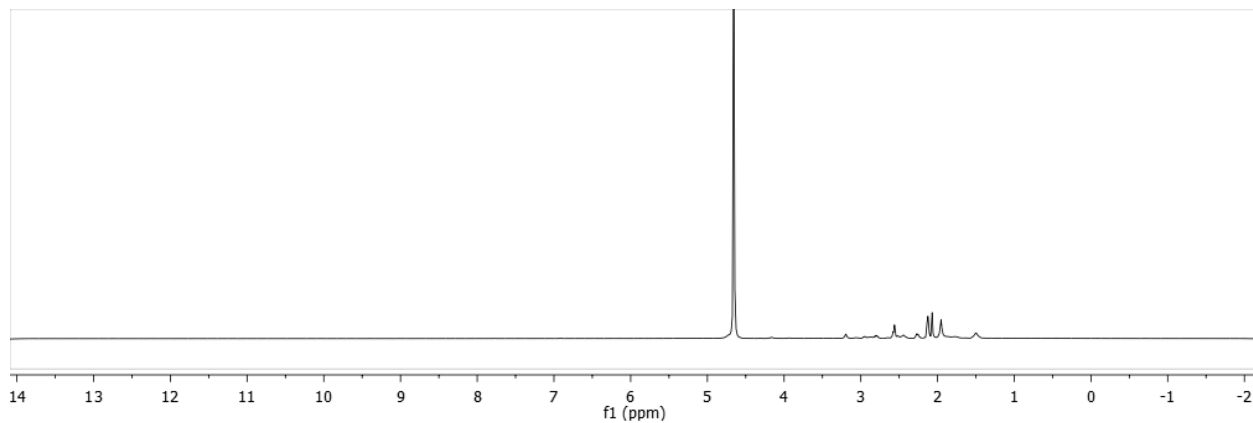
(actual) = 288.14406



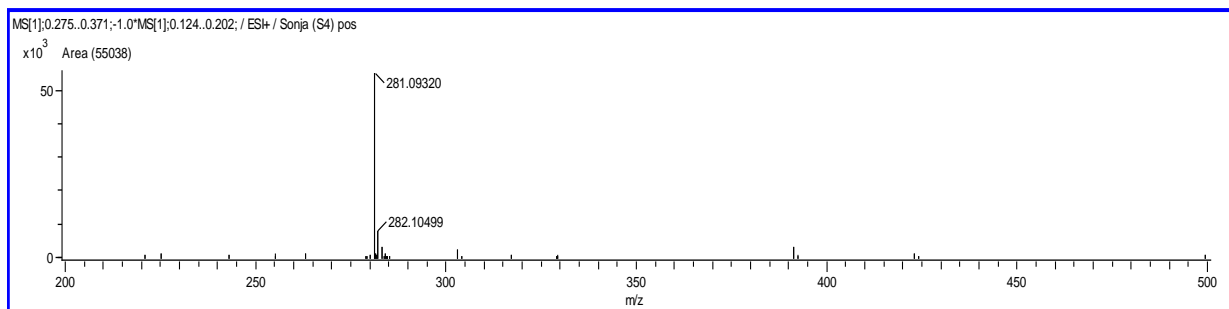
MS Diazo Diol (¹H NMR, ¹³C NMR)



MS DPD (Top) → Quinoxaline derivatization with phenylenediamine (Bottom)



[M+H]⁺ (expected) = 281.09600
(actual) = 281.09320



4.6 References

- ¹ Watanabe, T. (1963). Infective Heredity of Multiple Drug Resistance in Bacteria. *Bacteriol. Rev.* 27:87-115.
- ² Tenaillon, O. Erick Denamur, E., Matic, I. (2004). Evolutionary significance of stress induced mutagenesis in bacteria. *Trends in Microbiol.* 12(6): 264-269.
- ³ Walsh, C. (2000). Molecular Mechanisms That Confer Antibacterial Drug Resistance. *Nature* 406:775-781.
- ⁴ Sintim, H.O., Smith, J.A.I., Wang, J., Nakayama, S, Yan, L. (2010). Paradigm shift in discovering next-generation anti-infective agents: targeting quorum sensing, c-di-GMP signaling and biofilm formation in bacteria with small molecules. *Future Med. Chem.* 2:1005-1035.
- ⁵ Bassler, B.L. (1999). How bacteria talk to each other: regulation of gene expression by quorum sensing. *Curr. Opin. Microbiol.* 2:582–587.
- ⁶ Pirhonen, M., Flego, D., Heikinheimo, R., Palva, E.T. (1993). A small diffusible signal molecule is responsible for the global control of virulence and exoenzyme production in the plant pathogen *Erwinia carotovora*. *EMBO J.* 12(6):2467-2476
- ⁷ Davies, D.G., Parsek, M.R., Pearson, J.P., Iglewski, B.H., Costerton, J.W., Greenberg, E.P. (1998). The involvement of cell-to-cell signals in the development of a bacterial biofilm. *Science* 280(5361):295-298.

-
- ⁸ Davey, M.E., O'Ttoole, G.A. (2000). Microbial Biofilms: from Ecology to Molecular Genetics. *Microbiol. Mol. Biol. Rev.* 64(44):847-867.
- ⁹ Schuester, M., Lostroh, C.P., Ogi, T. Greenberg, E.P. (2003). Identification, timing, and signal specificity of *P. aeruginosa* Quorum-Controlled Genes: a Transcriptome analysis. *J. Bacteriol.* 85:2066-2079.
- ¹⁰ Whiteley, M., Parsek, M.R, Greenberg, E.P. (2000). Regulation of Quorum Sensing by *RpoS* in *Pseudomonas aeruginosa*. *J. Bacteriol.* 182(15) 4356-4360.
- ¹¹ Sperandio, V., Torres, A.G., Giron, J.A., Kaper, J.B. (2001). Quorum Sensing Is a Global Regulatory Mechanism in Enterohemorrhagic *Escherichia coli* O157:H7. *J. Bacteriol.* 183(17): 5187–5197.
- ¹² Wood, T.K. (2008). Insights on *Escherichia coli* biofilm formation and inhibition from whole-transcriptome profiling. *Environ. Microbiol.* 11(1):1-15.
- ¹³ Sperandio, V., Torres A.G., Kaper, J.B. (2002). E. coli Regulators B and C (QscBC): a Novel 2-component Regulatory System Involved in the Regulation of Flagella and Motility by Quorum Sensing in E. coli. *Mol. Microbiol.* 43(3): 809-821.
- ¹⁴ Choo, J., Shin, D., Ryu, S. (2007). Implication of QS in *Salmonella enterica* serovar *typhimurium* Virulence: the LuxS gene is Necessary for Expression of Genes in Pathogenicity Island I. *Infect. Immun.* 75(10): 4885-4890.
- ¹⁵ Yarwood, J.M., Bartels, D.J., Volper, E.M., Greenberg, E.P. (2004). Quorum Sensing in *Staphylococcus aureus* Biofilms. *J. Bacteriol.* 186(6):1838-1850.
- ¹⁶ Zhang, H.B., Wang, L.H., Zhang, L.H. (2002). Genetic control of quorum-sensing signal turnover in *Agrobacterium tumefaciens*. *Proct. Natl. Acad. Sci.* 99(7): 4638–4643.

-
- ¹⁷ Habash, M. (1999). Microbial biofilms: their development and significance for medical device-related infections. *J. Clin. Pharmacol.* 39(9):887-898.
- ¹⁸ Smith R.S., Iglewski, B.H. (2003). *Pseudomonas aeruginosa* quorum sensing as a potential antimicrobial target. *J. Clin. Invest.* 112(10):1460-1465.
- ¹⁹ Costerton, J.W., Stewart, P.S., Greenberg, E.P. (1999). Bacterial biofilms: a common cause of persistent infections. *Science* 284(5418):1318-1322.
- ²⁰ Oliver, A., Canton, R., Campo, P., Baquero, F., Blazquez, J. (2000). High Frequency of Hypermutable *Pseudomonas aeruginosa* in Cystic Fibrosis Lung Infection. *Science* 288:1251-1253.
- ²¹ Greenberg, E.P., Costerton, J.W., Iglewski, B.H, Pearson, J.P., Parsek, M.R., Davies, D.G. (1998). The Involvement of Cell-to-Cell Signals in the Development of a Bacterial Biofilm. *Science* 280:296-297.
- ²² Wood, T.K. (2009). Insights on Escherichia coli Biofilm Formation and Inhibition from Whole-Transcriptome Profiling. *Environ. Microbiol.* 11(1):1-15.
- ²³ Li, J., Attila, C., Wang, L., Wood, T.K., Valdes, J.J., Bentley, W.E. (2007). Quorum Sensing in Escherichia coli Is Signalled by AI-2/LsrR: Effects of Small RNA and Biofilm Architecture. *J. Bacteriol.* 189:6011-6020.
- ²⁴ Lerat, E., Moran, N.A. (2004). The Evolution of Quorum Sensing Systems in Bacteria. *Mol. Biol. Evol.* 21(5):903-913.

-
- ²⁵ Hauck, T., Hubner, Y., Bruhlmann, F., Schwab, W. (2003). Alternative pathway for the formation of 4,5-dihydroxy-2,3-pentanedione, the proposed precursor of 4-hydroxy-5-methyl-3(2*H*)-furanone as well as autoinducer-2, and its detection as natural constituent of tomato fruit. *Biochim. Biophys. Acta* 1623(2-3):109-119.
- ²⁶ Tavender, T.J., Halliday, N.M., Hardie, K.R., Klaus, W. (2008). LuxS Independent Formation of AI-2 from Ribulose-5-phosphate. *BMC Microbiol.* 8:98-100.
- ²⁷ Kong, P., Tyler, B.M, Richardson, P.A., Lee, B. W.K., Zhou, Z.S., Hong, C. (2010). Zoospore Interspecific Signalling Promotes Plant Infection By Phytophthora. *BMC Microbiol.* 10:313-316.
- ²⁸ Nichols, J.D., Johnson, M.R. (2009). Temperature, Not LuxS, Mediates AI-2 Formation in Hydrothermal Habitats. *FEMS Microbiol. Ecol.*, 68:173–181.
- ²⁹ Gonzalez, J.E., Keeshavan, N.D. (2006). Messing with Bacterial Quorum Sensing. *Microbiol. Mol. Biol.Rev.* 70(4):859-875.
- ³⁰ Moré M.I, Finger L.D, Stryker J.L, Fuqua C, Eberhard A, Winans S.C. (1996). Enzymatic synthesis of a quorum-sensing autoinducer through use of defined substrates. *Science* 272:1655–1658.
- ³¹ Fuqua C, Parsek M.R, Greenberg E.P. (2001). Regulation of gene expression by cell-to-cell communication: acyl-homoserine lactone quorum sensing. *Annu. Rev. Genet.* 35:439–468.
- ³² Bassler B.L, Wright M, Showalter R.E, Silverman M.R. (1993). Intercellular signaling in *Vibrio harveyi*—sequence and function of genes regulating expression of luminescence. *Mol. Microbiol.* 9: 773–786.

-
- ³³ Milton D.L, Chalker V.J, Kirke D, Hardman A, Cámara M, Williams P. (2001). The LuxM homologue VanM from *Vibrio anguillarum* directs the synthesis of N-(3-hydroxyhexanoyl)homoserine lactone and N-hexanoylhomoserine lactone. *J. Bacteriol.* 183: 3537–3547.
- ³⁴ Laue B.E, Jiang Y., Chhabra S.R., Jacob S., Stewart G.S.A.B., Hardman A., Downie J.A., O'Gara F., Williams P. (2000). The biocontrol strain *Pseudomonas fluorescens* F113 produces the *Rhizobium* small bacteriocin N-(3-hydroxy-7-cis-tetradecenoyl) homoserine lactone via HdtS, a putative novel N-acylhomoserine lactone synthase. *Microbiol.* 146:2469–2480.
- ³⁵ Ng, W. L. and Bassler, B. L. (2009). Bacterial quorum sensing network architectures. *Annu. Rev. Genet.* 43:197-222.
- ³⁶ Kaplan, H.B., Greenberg, E.P. (1985). Diffusion of autoinducer is involved in the regulation of the *Vibrio fischeri* luminescence system. *J. Bacteriol.* 163(3):1210-1214.
- ³⁷ Bassler, B.L., Wright, M.m Showalter, R.E., Silverman, M.R. (1993) Intercellular signaling in *Vibrio harveyi*: sequence and function of genes regulating expression of luminescence. *Mol. Microbiol.* 4:773-786.
- ³⁸ Henke, J.M., Bassler, B.L. (2004). Three parallel quorum sensing systems regulate gene expression in *Vibrio harveyi*. *J. Bacteriol.* 186 (20): 6902-6914
- ³⁹ Chen, X., Schauder, S., Potier, N., Van Dorsselaer, A., Pelczer, I., Bassler, B.L., and Hughson, F.M. (2002). Structural identification of a bacterial quorum-sensing signal containing boron. *Nature* 415, 545–549.

-
- ⁴⁰ Miller, S.T., Xavier, K.B., Campagna, S.R., Taga, M.E., Semmelhack, M.F., Bassler, B.L., Hughson, F.M. (2004) *Salmonella typhimurium* recognizes a chemically distinct form of the bacterial quorum sensing signal AI-2. *Mol. Cell* 15(5):677-687.
- ⁴¹ Mattmann, M.E., Blackwell, H.E. (2010). Small Molecules that Modulate Quorum Sensing and Control Virulence in *P. aeruginosa*. *J. Org. Chem.* 75(20):6737-6746.
- ⁴² Hentzer, M., Givskov, M. (2003). Pharmacological inhibition of quorum sensing for the treatment of chronic bacterial infections. *J. Clin Invest.* 112(9):1300–1307.
- ⁴³ Galloway, J.D., W.R, Hodgkinson, J.T., Bowden, S.D., Welch, M., Spring, D.R. (2011). Quorum Sensing in Gram-Negative Bacteria: Small-Molecule Modulation of AHL and AI-2 Quorum Sensing Pathways. *Chem. Rev.* 111:28–67
- ⁴⁴ Schaefer, A.L., Hanzelka, B.L., Eberhard, A., Greenberg, E.P. (1996). Quorum Sensing in *Vibrio Fischeri*: Probing Autoinducer-LuxR Interactions with Autoinducer Analogs. *J. Bacteriol* 178(10):2897.
- ⁴⁵ Eberhard A, Widrig CA, McBath P, Schineller JB. (1986). Analogs of the autoinducer of bioluminescence in *Vibrio fischeri*. *Arch Microbiol* 146:35–40.
- ⁴⁶ Smith, K.M., Bu, Y., Suga, H. (2003). Library Screening for Synthetic Agonists and Antagonists of a *Pseudomonas aeruginosa* Autoinducer. *Chem. Biol.* 10(6): 563–571
- ⁴⁷ Sun, J., Daniel, R., Wagner-Dobler, I., Zeng, A.P. (2004). Is autoinducer-2 a universal signal for interspecies communication: a comparative genomic and phylogenetic analysis of the synthesis and signal transduction pathways. *BMC Evol. Biol.* 4:36-47.

-
- ⁴⁸Lowery, C.A., Salzameda, N.T., Sawada, D., Kauffman, G.F., Janda, K.D. (2010). Medicinal Chemistry as a Conduit for the Modulation of Quorum Sensing. *J. Med. Chem.* 53(21):7467-7489.
- ⁴⁹ Miller, M.B., Karen, S., Lenz, D.H., Taylor, R.K., Bassler, B.L. (2002). Parallel Quorum Sensing Systems Converge to Regulate Virulence in *Vibrio cholerae*. *Cell* 110:303-314.
- ⁵⁰ Meijler, M.M., Hom, J.L., Kaufmann, G.F., McKenzie, M., Sun, C., Moss, J.A., Matsushita, M., Janda, K.D. (2004). Synthesis and Biological Evaluation of a Ubiquitous Quorum-Sensing Molecule. *Angew. Chem. Int. Ed.* 43:2106-2108.
- ⁵¹ Semmelhack, M.F., Campagna, S.R., Federle, M.J. Bassler, B.L. (2004). An Expedient Synthesis of DPD and Boron Binding Studies. *Org. Lett.* 7(4): 569-572.
- ⁵² De Keersmaecker, S.C.J., Varszegi, C., van Boxel, N., Habel, L.W., Metzger, K., Daniels, R., Marchal, K., De Vos, D., Vanderleyden, J. (2005). Chemical Synthesis of (S)-4,5-dihydroxy-2,3-pentadione, a Bacterial Signal Molecule Precursor, and Validation of its Activity in *Salmonella typhimurium*. *J. Biol. Chem.* 250(20): 19563-19568.
- ⁵³ Frezza M, Soullère L, Queneau Y, Doutheau A. (2005). A Baylis–Hillman/ozonolysis route towards (±) 4,5-dihydroxy-2,3-pentanedione (DPD) and analogues. *Tet Lett.* 46:6495–6498.
- ⁵⁴ Smith, J.A., Wang, J., Mau-Nguyen, S.M., Lee, V., Sintim, H.O. (2009). Biological Screening of a Diverse Set of AI-2 Analogs in *Vibrio Harveyi* Suggests That Receptors Which Are Involved in Synergistic Agonism of AI-2 and Analogs Are Promiscuous. *Chem. Comm.* 2009:7033-7035.

-
- ⁵⁵ Duan, K., Dammel, C., Stein, J., Rabin, H. & Surette, M. (2003). Modulation of *Pseudomonas aeruginosa* gene expression by host microflora through interspecies communication. *Mol. Microbiol.* 50: 1477–1491.
- ⁵⁶ Xavier, K.B., Miller, S.T., Lu, W., Kim, J.H., Rabinowitz, J., István Pelczar, I., Semmelhack, M.F., Bassler, B.L. (2007). Phosphorylation and Processing of the Quorum-Sensing Molecule Autoinducer-2 in Enteric Bacteria. *ACS Chem. Biol.* 2(2):128-136.
- ⁵⁷ Frezza, M., Soulere, L., Balestrino, D., Gohar, M., Deshayes, C., Queneau, Y., Forestier, C., Doutheau, A. (2007). Ac₂-DPD, the bis-(*O*)-acetylated derivative of 4,5-dihydroxy-2,3-pentanedione (DPD) is a convenient stable precursor of bacterial quorum sensing autoinducer AI-2. *Bioorg. Med. Chem.Lett.* 17(5):1428-143.
- ⁵⁸ Smith, J.A. (2011) The Synthesis of a Diverse Library of AI-2 analogs to Investigate Bacterial Quorum Sensing. Published doctoral dissertation, University of Maryland, College Park, Maryland.
- ⁵⁹ Taga, M.E., Semmelhack, J.L., Bonnie, B.L. (2001). The LuxS-dependent Autoinducer AI-2 Controls the Expression of an ABC Transporter That Functions in AI-2 Uptake in *Salmonella typhimurium*. *Mol. Microbiol.* 42(3): 777-793.
- ⁶⁰ O'Toole, G.A., Pratt, L.A., Watnick, P.I., Newman, D.K., Weaver, V.B., and Kolter, R. (1999). Genetic approaches to study of biofilms. *Methods Enzymol.* 310:91-109.

-
- ⁶¹ Rashid, M.H., Rumbaugh, K., Passadors, L., Davies, D.G., Hamood, A.N., Iglewski, B.H., Kornberg, A. (2000). Polyphosphate kinase is essential for biofilm development, quorum sensing, and virulence of *Pseudomonas aeruginosa*. *Proct. Nat'l. Acad. Sci.* 97(17):9636-9641.
- ⁶² Ganin, H., Tang, X, Meijler, M.M.(2009). Inhibition of *Pseudomonas aeruginosa* quorum sensing by AI-2 analogs. *Bioorg. Med. Chem. Lett.* 19(14):3914-3944.
- ⁶³ Alagely A. , Rajamani S. , Teplitski M.(2011) Luminescent Reporters and Their Applications for the Characterization of Signals and Signal-Mimics that Alter LasR-Mediated Quorum Sensing. *Springer Protocols* 692:113-130.
- ⁶⁴ Bottomley, M.J., Muraglia, E., Bazzo, R., Carfi, A. (2007). Molecular Insights into Quorum Sensing in the Human Pathogen *Pseudomonas aeruginosa* from the Structure of the Virulence Regulator LasR Bound to Its Autoinducer. *J. Biol. Chem.* 282(18):13592–13600
- ⁶⁵ Rye, C.S., Baell, J.B. (2005). Phosphate Isosteres in Medicinal Chemistry. *Curr. Med. Chem.* 12:3127-3144.
- ⁶⁶ Alagaely, A., Rajamani, S., Teplitski, M. (2011). Luminescent Reporters and their Applications for the Characterizations of Signals and Signal-Mimics that Alter LasR-Mediated Quorum Sensing. *Methods Mol. Biol.* 692(1):113-130.
- ⁶⁷ Miller, J. (1972). Experiments in Molecular Genetics, p. 352-355. Cold Spring Harbor Laboratory, NY.

⁶⁸ Trott, O., Olson, A.J. (2010). Autodock Vina: Improving the Speed and Accuracy of Docking With a New Scoring Function, Efficient Optimization and Multithreading. *J. Comp. Chem.* 31: 455-461.